We are IntechOpen,
the world's leading publisher of
Open Access books
Built by scientists, for scientists

6,900
Open access books available

186,000
International authors and editors

200M
Downloads

Our authors are among the

154
Countries delivered to

TOP 1%
most cited scientists

12.2%
Contributors from top 500 universities

CLARIVATE ANALYTICS
BOOK CITATION INDEX
INDEXED

WEB OF SCIENCE™

Selection of our books indexed in the Book Citation Index
in Web of Science™ Core Collection (BKCI)

Interested in publishing with us?
Contact book.department@intechopen.com

Chapter

Nanoprecipitation: Applications for Entrapping Active Molecules of Interest in Pharmaceutics

Oscar Iván Martínez-Muñoz, Luis Fernando Ospina-Giraldo and Claudia Elizabeth Mora-Huertas

Abstract

Nanoprecipitation technique, also named solvent injection, spontaneous emulsification, solvent displacement, solvent diffusion, interfacial deposition, mixing-induced nanoprecipitation, or flash nanoprecipitation, is recognized as a useful and versatile strategy for trapping active molecules on the submicron and nanoscale levels. Thus, these particles could be intended among others, for developing innovative pharmaceutical products bearing advantages as controlled drug release, target therapeutic performance, or improved stability and organoleptic properties. On this basis, this chapter offers readers a comprehensive revision of the state of the art in research on carriers to be used for pharmaceutical applications and developed by the nanoprecipitation method. In this sense, the starting materials, the particle characteristics, and the *in vitro* and *in vivo* performances of the most representative of these carriers, i.e., polymer, lipid, and hybrid particles have been analyzed in a comparative way searching for a general view of the obtained behaviors.

Keywords: nanoprecipitation, nanoparticles, colloidal carriers, drug delivery systems, lipid carriers, hybrid nanoparticles

1. Introduction

Nanoprecipitation is a technique to incorporate active molecules into colloidal drug delivery systems, patented by Fessi et al. [1, 2], which attracts attention for developing pharmaceutical products mainly due to the simplicity of its procedure [3]. The obtained particles enable the optimization of the drug *in vivo* therapeutic performance exhibiting, for example, controlled release behaviors, target delivery, and better stability in biological fluids, which means major mean residence times, half-lives increased, and more efficient addressing of the actives toward the different body tissues. Consequently, less toxicity and minor secondary effects are expected.

Some of the research works undertaken during the last years have proposed the vectorization in nanoparticles, via nanoprecipitation, of hydrophobic active molecules, mainly exhibiting logP values higher than 3. They include antineoplastics (e.g., doxorubicin [4], paclitaxel [5, 6], docetaxel [7, 8], methotrexate [9], triptolide [6], cucurbitacin [10], and sorafenib [11]), antiretrovirals (e.g., efavirenz [12] and

nevirapine [13]), immune suppressants (mycophenolate [14]), anti-inflammatories (clobetasol [15], fluticasone propionate [16], dexamethasone [17, 18], and diclofenac [19]), antimicrobial and antifungal agents (polymyxin B [20], amphotericin B [21], itraconazole [22], and linezolid [23]), antihyperlipidemics (fenofibrate [24, 25]), anesthetics (tetracaine [26] and ketamine [27]), antihypertensives (nimodipine [28] and atenolol [29]), vitamins or their precursors (β-carotene [30] and vitamin E [31]), and antioxidants (quercetin [14, 32]). Likewise, although in a much smaller number, hydrophilic active molecules such as alendronate [33], N-acetylcysteine [34], and calcein [35], have been investigated. Moreover, natural extracts such as Brazilian red propolis extract [36] and essential oils [37] have also been incorporated into polymeric nanoparticles.

Practical matters as the possibility to use solvents of low toxic potential, the simple procedure, the low energy consumption required, and the feasibility to obtain particles from diverse compositions are also highlighted among the pros of the nanoprecipitation method when carriers at the submicron and nanometric scales are intended [3, 38]. Most of the nanoparticulated drug delivery systems reported as prepared by nanoprecipitation have been developed by using the physicochemical principles governing this technique, primarily those who underpin the precipitation of materials from the mixture of a solvent/non-solvent for the involved material. They include in their majority, polymer, lipid, and hybrid nanoparticles; therefore, this review will be fundamentally focused on them. Nevertheless, some interesting developments of nanoparticles prepared by nanoprecipitation have been reported as well. For example, Arizaga et al. [39] and Villela et al. [40] entrapped magnetic nanoparticles inside polymeric particles, Fan et al. [41] designed spatially controlled release multistage carriers via the complexation of dendrimers with gelatin, and Allen et al. [35] entrapped hydrophobic and hydrophilic active molecules into polymersomes. Likewise, modifications to facilitate the industrial scaling-up of the preparation process have been investigated by Charcosset et al. [42] and D'Oria et al. [43] who developed procedures based on the use of a membrane contactor. On its part, Valente et al. [44] and Tao et al. [45] propose controllable mixing devices such as microfluidic mixer systems that allow continuous and scalable processes for the synthesis of the particles.

Reviews published to date dealing with the nanoprecipitation technique provide valuable information from different standpoints. For example, regarding the role of the obtained particles as drug delivery systems and their applications in medicine, Martínez et al. [46] highlighted their ability for carrying either natural products or actives obtained via chemical synthesis. On the other hand, with respect to the study of nanoprecipitation as a physicochemical process, Mora-Huertas et al. [47] revised the influence of both the formulation and the work conditions used to prepare nanoparticles. In this case, data available in scientific reports supplemented with a systematic study of the nanoprecipitation method led to an approximation to the particle formation mechanisms and identify the factors influencing the particle properties. Recently, Saad and Prud'homme [48] deepened on the physicochemical principles of the nanoparticle formation when amphiphilic block copolymers are used as stabilizing agents (named flash nanoprecipitation). They focused on the key variables determining the nucleation and growth phenomena related to the particle formation, particularly the supersaturation condition, the mixing step, and the used solvents and stabilizing agents.

Based on the above, the present chapter revises the generalities of the nanoprecipitation technique such as the physicochemical aspects involved, some of the starting materials used to obtain polymer, lipid, and hybrid nanoparticles, and their characteristics. Then, the pharmacokinetic behaviors, safety evaluations, and efficacy tests are analyzed. It is our interest to provide readers with a

comprehensive view about the nanoprecipitation as a technique to prepare nanocarriers and its potentialities for developing innovative pharmaceutical products.

2. Physicochemical fundamentals of the nanoprecipitation technique

To prepare nanoparticles via the nanoprecipitation technique, two miscible solvents are used, one of them being a good solvent (usually an organic solvent as ethanol, isopropanol, or acetone) and the other one acting as a non-solvent for the material that will form the particle (i.e., polymer, lipid, etc.), e.g., water. In general, as shown in **Figure 1**, the nanoprecipitation procedure requires the preparation of an organic phase and a non-solvent phase, frequently named aqueous phase, both guaranteeing the total solubility of all the starting materials. In this sense, the organic phase could contain polymers or solid and liquid lipids, surfactants of low HLB value, and active molecules dissolved in a solvent or mixture of organic solvents. The solubility in the solvent of the active molecule to be entrapped is one of the factors limiting the drug loading of the particles. On its part, the non-solvent phase mainly includes stabilizing agents solubilized in water, which allows the particle formation and the physical stability of the system [2]. Nonetheless, the preparation of particles without stabilizing agents has been reported. In these cases, for example, isoprenoid chains are linked to the active molecule making it easy to form the nanoparticle because of its amphiphilic nature [49].

Nanoparticles are spontaneously formed when the organic phase is dropped or added in a one-shot to the aqueous phase. Indeed, nanoprecipitation is a robust process and operational conditions used to prepare the particles do not seem to have a marked influence on the obtained particle size and polydispersity index. On the contrary, the variables linked to the used formulation appear as determinants of the characteristics of the nanosized system, mainly the nature and concentration of the starting materials [47]. This might be closely related to the proposed mechanisms to
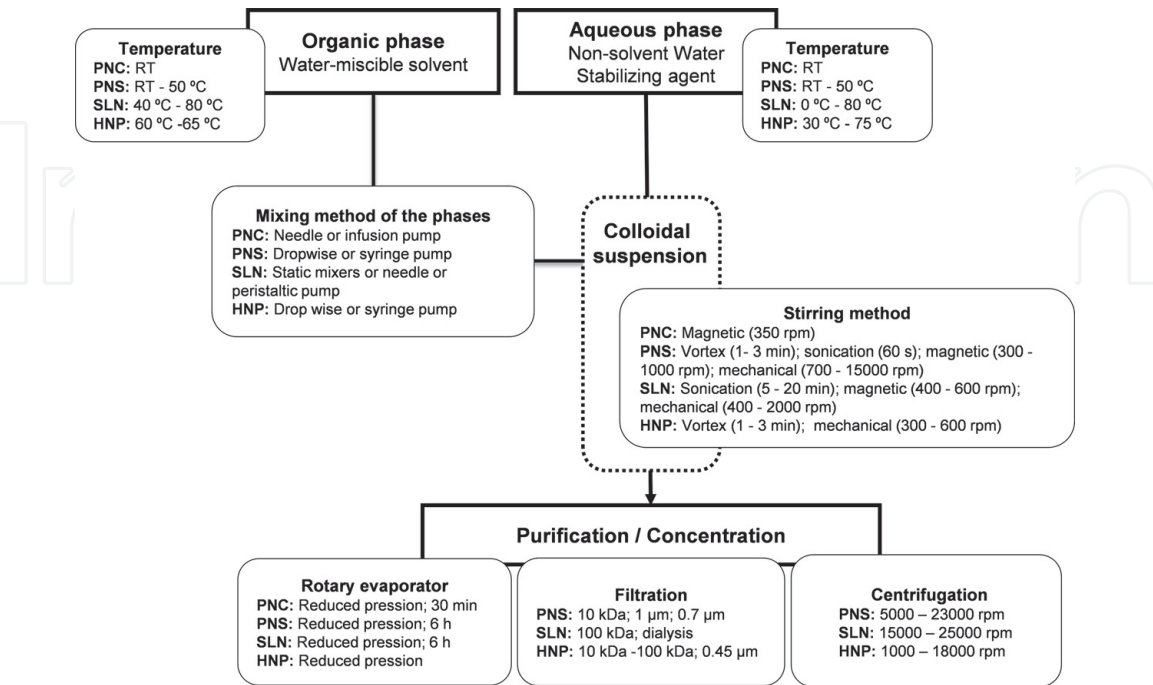

Figure 1.
General view of the preparation of polymer, lipid, and hybrid particles by nanoprecipitation summarizing the work conditions commonly reported (PNC: polymeric nanocapsules; PNS: polymeric nanospheres; SLN: solid lipid nanoparticles; HNP: hybrid nanoparticles; RT: room temperature).

form the particles by the nanoprecipitation technique. As a basic premise, only specific polymer/solvent/non-solvent ratios, where the polymer is in low concentrations and the solvent is in low proportion with respect to the nonsolvent, lead to particles at the nano- and submicron levels [50]. Thus, on the one hand, the mechanical approach states that when the phases are mixed, the organic phase is successively broken as drops within the aqueous phase due to the interfacial turbulence and thermal inequalities in the system because of the mutual miscibility between the solvent and the non-solvent and their different interfacial tensions (Gibbs-Marangoni effect) [51]. This fragmentation process will occur until the difference in interfacial tensions is minimized and the organic solvent migrates from the drops having a submicron size, which creates a non-solubility condition for the material causing the precipitation of the particles. On the other hand, a mechanism based on the chemical instability of the system has also been proposed ("ouzo effect"). In this case, when the phases are mixed, supersaturation of the molecules forming the particles is caused as the organic solvent migrates toward the aqueous phase, allowing the formation of "protoparticles" that grow following the classical nucleation-and-growth process [48, 52, 53]. It seems that depending on the formulation to prepare the nanoparticles, one of those mechanisms could predominate during the nanoprecipitation, and consequently, the adequate work conditions should be defined for allowing the spontaneous formation of submicron or nano-scale particle sizes exhibiting the smallest polydispersity indexes. Difficulties associated with the standardization of the procedure of nanoprecipitation result in the polymer aggregation yielding wide and asymmetric particle size distributions. For example, polymer aggregates are evidenced because of a concentrated organic phase, high organic phase ratio, low concentration of stabilizing agent, and poor mixing of the phases [47].

It is worth clarifying that in-depth studies on how particles are formed via the nanoprecipitation technique and the operating variables determining their characteristics have been carried out by using polymeric systems. Regarding lipid nanoparticles, only systematic studies have been reported to aid in understanding the variables that influence the preparation of the carriers; among them, the contributions of Martínez-Acevedo et al. [54] on the influence of the used recipe and Noriega-Pelaez [55] on the study of the particle preparation process are highlighted. Concerning the hybrid particles, research works to date have focused primarily on the impact of the starting materials on the particle characteristics [5, 9, 12, 23, 56].

Once the nanocarriers are formed, the particle dispersions are further processed to purified and concentrate them. To this end, rotary evaporation [14, 18, 22–24, 31, 55] and centrifugation [5, 6, 12, 13, 15, 16, 23, 25, 27–29, 36, 56, 57] are the most used methods; however, filtration [4, 6, 16, 18, 24] and dialysis [7–9, 21, 27, 34] have also been reported. Likewise, lyophilization is the preferred technique to stabilize the nanoparticles, although the storage to low temperatures has been used to preserve the aqueous dispersions [5, 8, 9, 13, 21, 29].

3. Starting materials and general characteristics of particles prepared by nanoprecipitation

As mentioned above, although different types of carriers intended for pharmaceutical applications can be prepared via nanoprecipitation, only polymer, lipid, and hybrid particles were chosen to be analyzed in detail because of the amount of reported research works to date. Polymeric nanoparticles are classified as polymeric nanospheres (PNS) and polymeric nanocapsules (PNC). The first ones correspond to a solid matrix conformed by the used polymers and other components, e.g.,

active molecules and lipophilic surfactants. On its part, the structure of the nanocapsules is proposed as an oil core surrounded by a polymeric shell. Approximately, 90% of the research works published on the preparation of polymeric nanoparticles via the nanoprecipitation technique are devoted to the obtention of nanospheres.

With respect to lipid nanoparticles, both solid lipid nanoparticles (SLN) and nanostructured lipid carriers (NLC) have been investigated, although almost 85% of the research works deal with SLN. Lipids nanoparticles are composed of a lipid matrix that is supposed to be surrounded by stabilizing agents. In the case of SLN, the lipid matrix is exclusively formed by solid lipids, while the lipid matrix of NLC is composed of solid and liquid lipids. It seems that the liquid lipid in NLC favors the entrapment efficiency of the active molecules [58].

Regarding hybrid nanoparticles, they are made from both polymers chemically modified with lipids (e.g., 1,2-distearoyl-sn-glycero-3-phosphoethanolamine-N-methoxy polyethylene glycol—DSPE-PEG) or the physical mixture between polymers and lipid components (e.g., PLGA and soy lecithin). Nevertheless, in the latter case, although the qualitative recipe is similar to that for polymeric particles, higher concentrations of solid lipids are used to prepare hybrid particles (i.e., lipid concentrations range between 20 and 50% for hybrid particles and between 1 and 5% for polymeric nanoparticles).

3.1 Starting materials

Figure 2 shows in a comparative way the reported starting materials used to prepare the different types of particles via nanoprecipitation. As can be seen, PLGA, PCL, and PLA are the most used polymers to prepare polymeric nanoparticles and when these polymers are chemically modified with, for example, PEG, stealth polymeric nanoparticles can be obtained [16, 17, 27]. Surfactants of low HLB value, e.g., soy phospholipids, could be added to the organic phase for facilitating the particle formation [19, 31] and, if nanocapsules are intended, castor oil, sesame oil, caprylic capric triglycerides, and caprylic capric triglyceride PEG-4 esters are part of the organic phase. Acetone appears as the preferred organic solvent of the organic phase and the non-solvent is water. Thus, the aqueous phases are solutions of stabilizing agents as poloxamer, polyvinyl alcohol, and polysorbate 80, which prevent the particle aggregation phenomena. Likewise, aqueous phases can only be water [16] or phosphate buffer [27, 59].

To prepare SLN, fatty acids and their glyceryl esters are frequently used as lipids (e.g., glyceryl monostearate, tristearate, behenate, and dilaurate); they are dispersed at a molecular level in organic solvents such as acetone and ethanol for obtaining the organic phase. As in the case of polymeric nanoparticles, phospholipids can be used to favor the particle formation and, to make NLC, liquid lipids as caprylic capric triglycerides are also dissolved in the organic phase. With respect to the non-solvent phase, aqueous solutions of stabilizing agents of varied nature are reported. Among them, surfactants as those mentioned for polymeric nanoparticles, proteins such as sodium caseinate and lactoferrin, and osmotic active compounds such as glucose and magnesium sulfate have been investigated.

Hybrid nanoparticles were designed to integrate the favorable characteristics of both polymeric and lipid systems and overcome their drawbacks [34]. These systems are proposed as an inner polymeric core surrounded by a lipid shell [60]. To obtain it, as is the rule in nanoprecipitation, organic and aqueous phases are designed so that solubility of the starting materials is guaranteed. As one of the strategies to prepare hybrid particles is employing polymers chemically modified with lipids (e.g., DSPE-PEG-NH2), they behave as amphiphilic compounds that
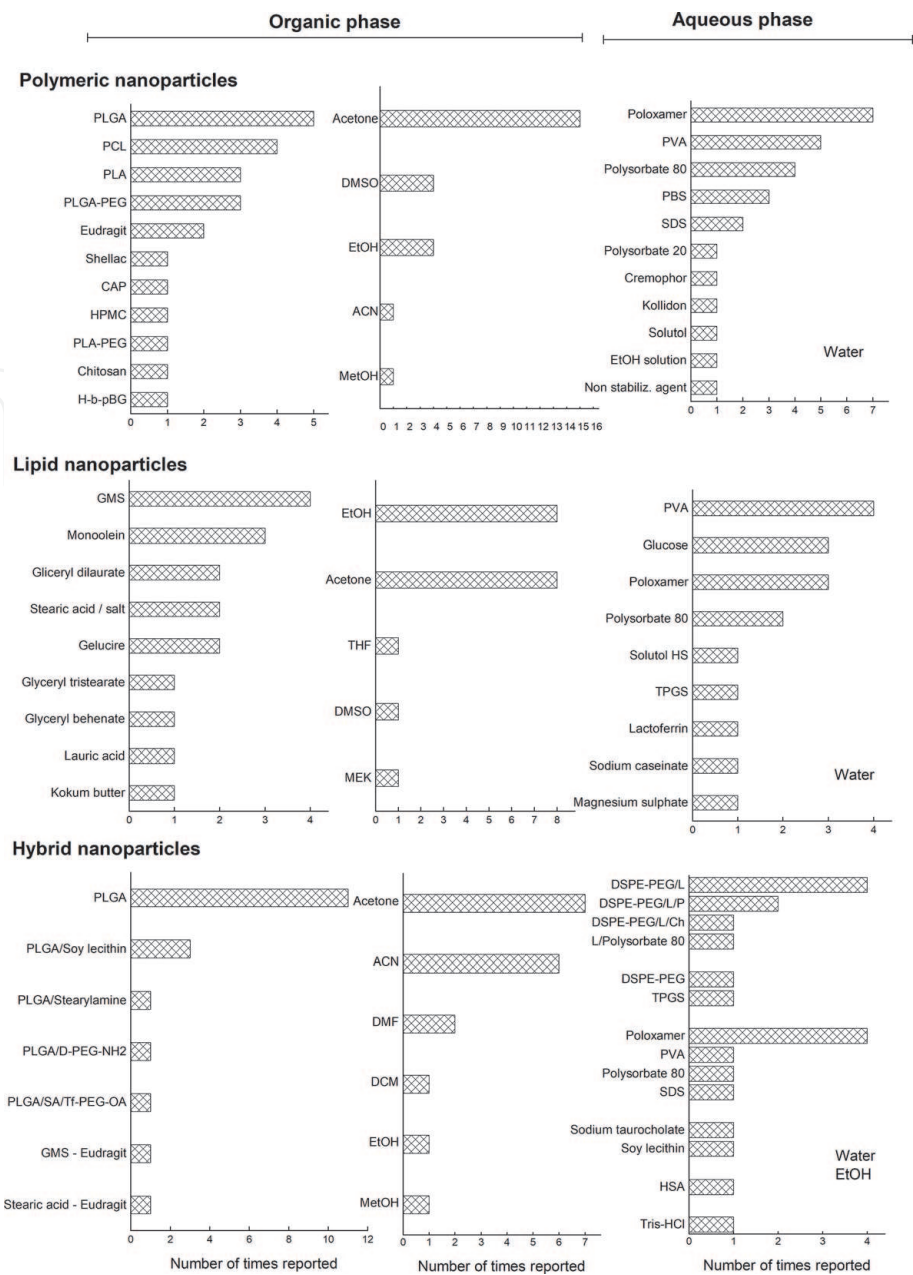
Figure 2.
Starting materials reported as used to prepare the organic and aqueous phases for obtaining polymer, lipid, and hybrid nanoparticles by the nanoprecipitation technique. Number of times reported for each starting material considering a total of 18, 11, and 13 research works for polymer, lipid, and hybrid particles, respectively [PLGA: poly(lactic-co-glycolic acid); PCL: polycaprolactone; PLA: poly(lactic acid); PEG: polyethylene glycol; HPMC: hydroxypropyl methylcellulose; DMSO: dimethyl sulfoxide; CAP: cellulose acetate phthalate; EtOH: ethanol; ACN: acetonitrile; MetOH: methanol; DMF: dimethylformamide; DCM: dichloromethane; THF: tetrahydrofuran; MEK: methyl ethyl ketone; H-b-pBG: hyaluronan poly(γ-benzyl-L-glutamate); PBS: phosphate-buffered saline; SDS: sodium dodecyl sulfate; GMS: glycerol monostearate; TPGS: tocopheryl polyethylene glycol succinate; PVA: polyvinyl alcohol; Tf-PEG-OA: transferrin-poly(ethylene glycol)-oleic acid; Tf: transferrin; HSA: human serum albumin; DSPE-PEG: 1,2-distearoyl-sn-glycero-3-phosphoethanolamine-N-[methoxy(polyethylene glycol)]].

could form part of any of the phases according to their solubility. On the contrary, if a physical mixture of polymer and lipid is used, they are dissolved in the organic phase. Unlike polymeric and lipid particles, acetonitrile is reported as the most used organic solvent for preparing hybrid nanoparticles. Another interesting matter of the recipe to prepare hybrid nanoparticles is the versatile composition of the aqueous phase. In this sense, for example, lecithin and cholesterol can be dissolved in ethanol and then incorporated in the aqueous phase that could contain surfactants such as polysorbate and poloxamer. Likewise, dispersions of surfactants, proteins, or buffers were tested as the aqueous phase.

3.2 General characteristics of the particles

Regardless of the type of particle, the shape, the particle size, the drug entrapment, and loading, and the zeta potential are among the crucial properties determining their pharmaceutical performance [61].

3.2.1 Shape

Polymeric and hybrid particles prepared by using the nanoprecipitation technique exhibit spherical shape as it is revealed by techniques of microscopy, mainly scanning electron (SEM), transmission electron (TEM), atomic force (AFM), and field emission scanning microscopies (FESEM). To investigate the shape of lipid nanoparticles in most cases, the same techniques were used, and spherical shapes were also reported. However, lipids might be melted during the sample examination destroying their native characteristics; consequently, controversial results could be obtained. For example, platelet shapes for SLN [62, 63] and structures with the liquid lipid located on the surface of the particles in the form of plates for NLC [64, 65] have been reported by using cryo-TEM and freeze-fracture TEM. Nevertheless, Dong et al. [24] report spherical shape from the analysis of SLN by using Cryo-FESEM.

3.2.2 Particle size

In general, the mean sizes, usually measured by dynamic light scattering, vary between less than 100 and 300 nm with PDI values below 0.4 (**Figure 3A** and **B**). It seems that polymeric nanocapsules and specially hybrid nanoparticles are the smallest; perhaps, any type of structural arrangement among the lipids and polymers could favor a better consolidation of the particle. With respect to lipid carriers, the platelet shapes as the lipids crystallize inside the particle could explain their high polydispersity [66].

3.2.3 Drug entrapment efficiency

Regarding the entrapment efficiency (**Figure 3C**), clear differences are identified among the carriers. Thus, polymeric nanocapsules entrap almost the totality of the active molecule in contrast with 40% attained by the SNL. As remarked by Westesen et al. [67], Pardeike et al. [68], and Weber et al. [69], when preparing SLN the solidification and the progressive crystallization of the lipid in more stable forms could lead the expulsion of the active substances whether during the particle formation or its consolidation. This results in eventual instabilities of the particle dispersions and, as evidenced in this case, low entrapment efficiency and loading of active molecules. On the other hand, as shown in **Figure 3D**, the best results of drug loading are reported for hybrid nanoparticles; active molecules could be located both in the polymeric core and the lipid layer of the particles maximizing their loading efficiency.

3.2.4 Physicochemical stability

Stability of the particle dispersions has been investigated by using refrigerated storage [6, 8, 13, 15, 21], room temperature at 25°C [8, 13, 14, 21, 57], and accelerated conditions varying between 35 and 40°C [8, 9, 11, 20, 27]. Particle size, PDI, and zeta potential are usually followed during the storage time, and the physical integrity of the dispersions is observed for up to 6 months. This good stability is expected for these nanosystems considering their colloidal nature and the absolute zeta potential values which are estimated varying between 15 and 40 mV.
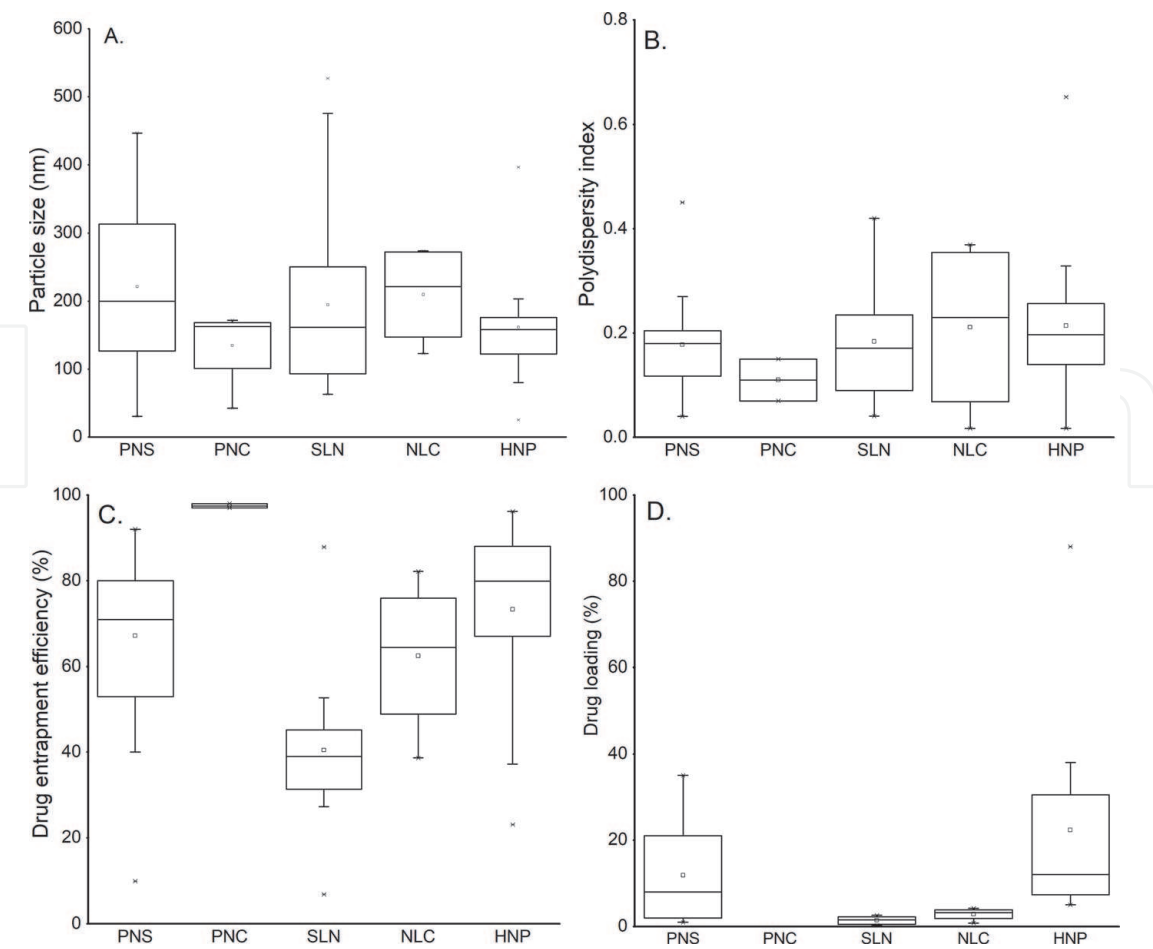
Figure 3.
General behaviors of particle size (A), polydispersity index (B), drug entrapment efficiency (C), and drug loading (D) for polymeric nanospheres (PNS), polymeric nanocapsules (PNC), solid lipid nanoparticles (SLN), nanostructured lipid carriers (NLC), and hybrid nanoparticles (HNP).

3.2.5 Release behavior

Table 1 summarizes the reported work conditions used to carry out the release tests. No matter what type of particles, dialysis is the most used technique to investigate their drug release behaviors, usually at 37°C in PBS media of pH 6.8 or 7.4. Comparisons of drug release data is risked because significant changes in the delivery behaviors are caused by the type of particle and its composition, the nature of the active molecule, and the work conditions associated with the release test, however, worth the risk for gaining a general view.

Thus, even though the mathematical modeling of the drug release data reported for the carriers of interest predicts Higuchi and Korsmeyer-Peppas kinetics, differences in the drug release patterns of polymeric, lipid, and hybrid particles are evidenced (**Figure 4**). In this way, biphasic release behaviors seem to be characteristic when nanoprecipitated polymeric particles, whether nanospheres or nanocapsules, are investigated. In these cases, the equilibrium is reached after 20 or 30 h of begun the study, and drug concentrations varying from 60 to 80% are released. Paclitaxel-loaded PLGA nanoparticles are the exception; in this case, a slow and constant drug release process occurs delivering hardly 40% of the active encapsulated after 60 h. Perhaps, the low entrapment efficiency of this molecule into the carriers makes the diffusion phenomena related to the active molecule delivery (37–70%) difficult.

On its part, the drug release patterns observed when lipid nanoparticles are tested seem to be those where the active molecule has faster delivery (before the

Nanoparticle	Drug release study				Reference
	Method	Medium	Stirring	Operating conditions	
Polymeric nanoparticles					
PNC	Directly added at the release medium	pH 6.8 PBS	Magnetic 25 rpm	37± 2°C	[19]
PNS	USP Apparatus I	pH 6.8 PBS	Mechanical 100 rpm	37± 2°C	[33]
PNS	Franz diffusion cells (sheep nasal mucosa)	pH 6.4 PBS	100 rpm	37± 0.5°C	[57]
PNS	Dialysis 12–14 kDa	pH 7.4 PBS	Mechanical 100 rpm	37± 1°C	[29]
PNS	Directly added at the release medium/ centrifugation	pH 7.4 PBS with 0.5% w/v polysorbate	Eppendorf thermomixer, gentle stirring	37°C	[16]
PNS	Dialysis	pH 7.4 PBS	Magnetic 100 rpm	37°C	[17]
PNS	Franz diffusion cells (dialysis 12–14 kDa)	pH 7.5 PBS	Magnetic 600 rpm	32°C	[18]
PNS	Dialysis 14 kDa	pH 7.4 PBS	Shaker 100 rpm	37± 2°C	[26]
PNS	Dialysis 10 kDa	pH 7.4 PBS	100 shakes/min	37°C	[27]
Lipid nanoparticles					
SLN/NLC	Directly added at the release medium	1% wt SDS solution	Shaker 60 strokes/min	37± 2°C	[15]
SLN/NLC	Directly added at the release medium/ centrifugation	0.2% wt SDS solution	Shaker 60 strokes/min	37± 2°C	[28]
SLN	Dialysis 50 kDa	pH 7.4 PBS	Shaker 50 rpm	37± 2°C	[24]
SLN	Dialysis 14 kDa	pH 7.4 PBS	Shaker 100 rpm	37± 2°C	[26]
SLN	Dialysis/USP Apparatus II	pH 7.4 PBS	Mechanical 100 rpm	37± 2°C	[13]
Hybrid nanoparticles					
HNP	Dialysis 3.5 kDa	pH 7.4 PBS	Gentle stirring	37 °C	[33]
HNP	Dialysis 12–14 kDa	pH 6.8 PBS (0.1 M)	Shaker 90 rpm	37 ± 2°C	[12]
HNP	Dialysis 10–12 kDa	pH 7.4. PBS with 0.1% (v/v) DMF	150 rpm	37 ± 0.5°C	[9]
HNP	Dialysis 12 kDa	pH 7.4 PBS	Shaker 100 rpm	37 ± 2°C	[4]
HNP	Dialysis 3.5 kDa	pH 7.4 PBS	100 rpm	37 °C	[6]
HNP	Dialysis 8–14 kDa	pH 7.4 PBS with 0.5% polysorbate 80	100 rpm	37°C	[56]
HNP	Dialysis 10 kDa	pH 7.4; 6.8 and 5.5 PBS	100 rpm	37 ± 1°C	[8]
HNP	Dialysis 12 kDa	pH 7.4 PBS	nr.	37 °C	[14]
HNP	Dialysis 100 kDa	pH 6.8 PBS, water, and HCl 0.1 M solution	nr.	nr.	[32]

Nanoparticle	Drug release study				Reference
	Method	**Medium**	**Stirring**	**Operating conditions**	
HNP	Dialysis 12 kDa	pH 7.4 PBS	Magnetic 200 rpm	$37 \pm 2°C$	[5]
HNP	Dialysis 10 kDa	pH 7.4 PBS	nr.	37 °C	[23]
HNP	Dialysis 10–12 kDa	PBS with pH 7.4 FBS (10%)	100 rpm	37°C	[11]

PNS: polymeric nanospheres; PNC: polymeric nanocapsules; SLN: solid lipid nanoparticles; NLC: nanostructured lipid carriers; HNP: hybrid nanoparticles; SDS: sodium dodecyl sulfate; DMF: dimethylformamide; PBS: phosphate buffer solution; FBS: fetal bovine serum; nr.: non-reported data.

Table 1.
Summary of the work conditions used to investigate the drug release behavior of nanoparticles prepared by the nanoprecipitation technique.
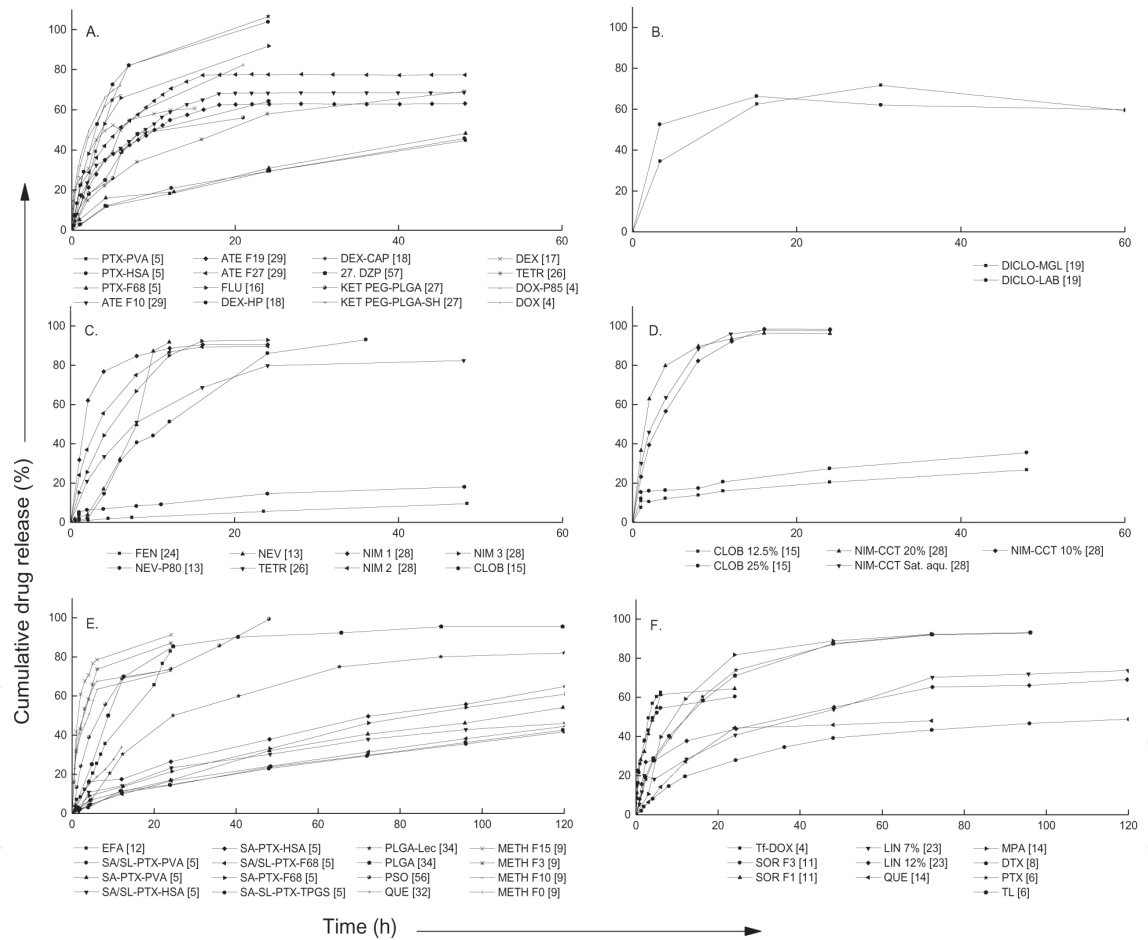

Figure 4.
Drug release behaviors for polymeric nanospheres (A), polymeric nanocapsules (B), solid lipid nanoparticles (C), nanostructured lipid carriers (D), hybrid nanoparticles obtained from the mixture of polymers and lipids (E), and hybrid nanoparticles obtained from chemically modified polymers with lipids (F) (PTX: paclitaxel; PVA: polyvinyl alcohol; ATE: atenolol; F: formulation; DEX: dexamethasone; CAP: cellulose acetate phthalate; HSA: human serum albumin; DZP: diazepam; TETR: tetracaine; F68: Pluronic 68; FLU: fluticasone propionate; KET: ketamine; SH: shellac; DOX: doxorubicin; P85: Pluronic 85; DICLO: diclofenac; MGL: Miglyol 810; LAB: labrafac; FEN: fenofibrate, NEV: nevirapine; NIM: nimodipine; P80: polysorbate 80; CLOB: clobetasol propionate; CCT: caprylic/capric triglycerides; EFA: efavirenz; SA: stearylamine, SL: soy lecithin; Lec: lecithin; METH: methotrexate; PSO: psoralen; TPGS: tocopheryl polyethylene glycol succinate; QUE: quercetin; Tf: transferrin; SOR: sorafenib; LIN: linezolid; DTX: docetaxel; MPA: mycophenolate; TL: triptolide).

first 20 h) and, at a rate, higher than 80%. Nimodipine reached delivered concentrations near 100% at 10 h, and other molecules such as tetracaine and nevirapine exhibit biphasic behaviors reaching drug deliveries higher than 80% at 25 h. NLC

appear to be more efficient than SLN during the release process. The highest amounts of active molecule that could be encapsulated because of the oil component in the particle structure might have influence. Once again, there are exceptions to the general behavior. In this way, slow-release processes as in the case of clobetasol and fenofibrate, lead to less than 40% of active molecule released even at 100 h. It is important to keep in mind that fenofibrate has a high logP value (~5.2) and that clobetasol propionate was the starting material to prepare the nanoparticles. Thus, a high affinity of the active molecules for the lipid matrix of the particle would difficult its delivery process.

Hybrid nanoparticles, irrespective of whether the particles are obtained from the mixture of polymers and lipids (**Figure 4E**) or by using chemically modified polymers with lipids (**Figure 4F**), characterize by a very slow release of the active molecule where, for example, some carriers deliver above 90% of the drug after 50 h of started the test. It should be noted that in this case, the data are reported twice the set time for the other carriers. For some active molecules such as methotrexate, N-acetylcysteine, psoralen, quercetin, and paclitaxel, the prolonged drug release could be related to the uniform distribution presumed for the drug into the matrix and the core-shell structure of the particle, which difficult the diffusion of the drug toward the release medium [9]. Likewise, the hydrolysis and erosion processes of the polymeric core could be hindered by the lipid layer surrounding the polymeric core [34] or, perhaps, the hydrophobic interactions of the active molecule with the polymer might result of relevance for the drug release [5]. These effects offset, for example, the favorable solubility gained because of the precipitation of amorphous active during the preparation of the particles, which is expected to facilitate the drug delivery [9].

4. *In vivo* performance of carriers prepared by nanoprecipitation

Drug delivery systems such as the polymeric, lipid, and hybrid nanoparticles have been promoted for use in therapeutics as an interesting approach to facilitate uptake of drugs at the desired site of action, particularly when free drugs might give rise to significant off-site toxicities or characterize by poor bioavailability because of their molecular and physicochemical properties. Accordingly, knowing the bioavailability behaviors, including the pharmacokinetic parameters and the biodistribution of the carriers obtained via the nanoprecipitation technique, as well as the stability of the carriers in biological fluids and their cellular uptake, result of paramount importance to investigate their applicability in pharmaceutics.

Considering that submicron sizes for most particles prepared by nanoprecipitation range between 200 and 300 nm, which are larger than pores between endothelial cells, it is expected that, in the absence of specific affinity for receptors, their distribution is limited to the vascular space. Nevertheless, for example, larger endothelial pores such as the fenestrations in the liver and the spleen might lead to the uptake of the particles by these tissues via bulk fluid flow. Once in the bloodstream, particles are coated with a layer of plasma proteins (opsonization or protein corona formation) facilitating their elimination by immune cells. Besides, dynamic interactions between nanoparticles and blood cells, e.g., erythrocytes, platelets, and leukocytes, could occur. Then, the carriers are entrapped in the microvasculature and clearing compartments of the reticuloendothelial system like the liver, the spleen, the bone marrow, and the lung, via phagocytic uptake by cells accessible from the vascular space such us the hepatic Kupffer cells. This allows the elimination of the particles from the organism via the bile ducts into the feces or in the urine [70].

To provide a therapeutic response, nanoparticles must overcome these physiological clearance mechanisms and distributional barriers. The objective is to guarantee a high mean residence time for the carriers in the systemic circulation while their drug release delivery is modulated. Some alternatives in this way include the development of particles exhibiting sizes less than 100 nm or a positive surface charge. Stealth particles by using nonionic polymers or mimic the outer surface of blood cells by locating mixtures of phospholipids, cholesterol, sphingomyelin, and ganglioside molecules on the particle surface have also been proposed, and the modification of the particle surface with specific ligands appears as the best strategy for the target delivery of active substances up to now [61, 70].

Regarding the carriers prepared by nanoprecipitation, among the reported developments of particles that could theoretically allow them a better *in vivo* performance are: (i) particle sizes lesser than 100 nm for polymeric nanospheres [25, 26, 34], solid lipid nanoparticles [71], and hybrid nanoparticles [7, 34, 56], (ii) positively charged polymeric nanospheres by using chitosan [72] and Eudragit® RL 100 [18] as polymers or positively charged hybrid nanoparticles prepared from lipids as the stearylamine [5], (iii) stealth polymeric nanospheres [17, 27] and stealth hybrid particles [4–8], and (iv) targeted cancer hybrid particles [7, 59].

4.1 Pharmacokinetic parameters

An approach to the pharmacokinetic aspects of the particles prepared via nanoprecipitation is made from the reported studies where carrier dispersions were administered by the intravenous, oral, and intranasal routes to animal models as Sprague-Dawley rats, Wistar rats, and BALB/c mice (**Table 2**). First, the slow-release patterns previously discussed appear to be maintained in the *in vivo* behavior, i.e., nanoparticles extend in some way the drug delivery regardless of the administration route and the carrier properties. Thus, mean residence times (MRT) in the systemic circulation between 1.2 and 20 folds higher than that for the free drug and elimination half-lives between 5 and 10 folds higher than free drug are achieved. Likewise, larger values of area under curve (AUC) are reported which, provided that the amount of drug that is released allows the therapeutic dose required, are attractive for treating chronic diseases where less frequent dosing regimens are convenient.

A general view depending on the administration route (**Figure 5**, where solid and dashed lines correspond to carriers and free-drug plasma profiles, respectively) shows that polymeric particles orally administered increase the T_{max}, C_{max}, and AUC_{0-t} values compared with free drugs administered in suspension or, as in the case of lipid nanoparticles, with an intravenously administered solution of the drug. The slow drug release behavior characteristic of lipid particles, where T_{max} is abruptly reached after 20 h of administration is interesting. On the other hand, although T_{max}, C_{max} and, AUC are increased when using hybrid particles, it must be noted that drug could be rapidly or slowly delivered to the serum which might be related to the location of the active molecule into the particle. For example, if the active molecule is located at the lipid shell surrounding the polymeric core, the drug might be easily released; on the contrary, if the active molecule locates at the polymeric core, more extended drug release behaviors could be obtained. Zhu et al. [4] and Godara et al. [5] demonstrate the usefulness of the lipid layer covering the polymeric core in the hybrid particles to prolong the circulation time of the particles. Probably, the lipid shell restricts the plasma protein adsorption reducing the opsonization phenomena. Moreover, the modifications of the particle with cholate enhance the drug absorption by the oral route. Likewise, developments as that of mycophenolate particles containing quercetin, where the antioxidant activity of

Active molecule—carrier	Active ingredient	Route of administration	Animal model	Equivalent dose of active molecule	T_{max} (h)	C_{max}	AUC_{0-t}	MRT (h)	$t_{1/2}$ (h)	Reference
Polymeric nanoparticles										
PNS	Itraconazole	Parenteral	Sprague-Dawley rats	5 mg/kg	7.7	nr.	1.2 µg h/mL	12.4	nr.	[22]
PNS (PEG-PLGA)	Ketamine	Parenteral	Male C57BL/6 J mice	1 mg/kg	nr.	20.1 µg/mL	88.6 µg h/mL	nr.	103.1	[27]
PNS (PEG-PLGA:SH)					nr.	19.6 µg/mL	86.8 µg h/mL	nr.	79.7	
PNS	Paclitaxel	Oral	Wistar rats	10 mg/kg	6.0	3.6–4.2 µg/mL	nr.	nr.	nr.	[5]
PNS	Diazepam	Intranasal	Sprague-Dawley rats	0.2–0.25 mg/kg	2.0	2.4%/g	13.9% h/g	nr.	nr.	[57]
Lipid nanoparticles										
SLN (P80)	Nevirapine	Parenteral	Wistar rats	20 mg/kg	4.0	9.3 µg/g	2.9 µg h/g	17.4	27.6	[13]
SLN					4.0	5.8 µg/g	1.1 µg h/g	8.6	7.2	
SLN	Amphotericin B	Oral	Sprague-Dawley rats	3.6 mg/kg	24.0	1.1 µg/mL	27.9 µg h/mL	nr.	15.9	[21]
Hybrid nanoparticles										
HNP	Doxorubicin	Parenteral	Male Sprague-Dawley rats	20 mg/kg	nr.	17.5 µg/mL	62.9 µg h/mL	9.5	6.4	[4]
HNP (P85)					nr.	17.8 µg/mL	75.4 µg h/mL	10.82	7.1	
HNP (Tf-P85)					nr.	19.9 µg/mL	107.1 µg h/mL	11.43	8.0	
HNP	Docetaxel	Parenteral	BALB/c female mice	10 mg/kg	nr.	8.0 µg/mL	198.5 µg h/mL	34.9	25.7	[8]
HNP	Mycophenolate	Oral	Sprague-Dawley rats	25 mg/kg equivalent to MPA and QC	nr.	1.2 µg/mL	27.4 µg h/mL	34.0	24.1	[14]
HNP	Mycophenolate + quercetin				nr.	1.2 µg/mL	35.9 µg h/mL	46.0	28.4	
HNP	Quercetin	Oral	Sprague-Dawley rats	25 mg/kg	1.0	8.8 µg/mL	33.3 µg h/mL	nr.	3.4	[32]
HNP	Paclitaxel	Oral	Wistar rats	10 mg/kg	6.0	6.8–7.6 µg/mL	nr.	nr.	nr.	[5]

PNS: polymeric nanospheres; SLN: solid lipid nanoparticles; NLC: nanostructured lipid carriers; HNP: hybrid nanoparticles; Tf: transferrin; P85: Pluronic 85; T_{max}: time taken to reach peak plasma concentration; $t_{1/2}$: half-life; C_{max}: maximum concentration; AUC_{0-t}: area under the curve of a plasma concentration versus time profile; MRT: mean residence time; P80: polysorbate 80; PEG: poly(ethylene glycol), PLGA: poly (D,L-lactic-coglycolic acid), SH: shellac, nr.: non-reported data.

Table 2.
Summary of the pharmacokinetic parameters reported in research works on nanoparticles prepared by the nanoprecipitation technique.
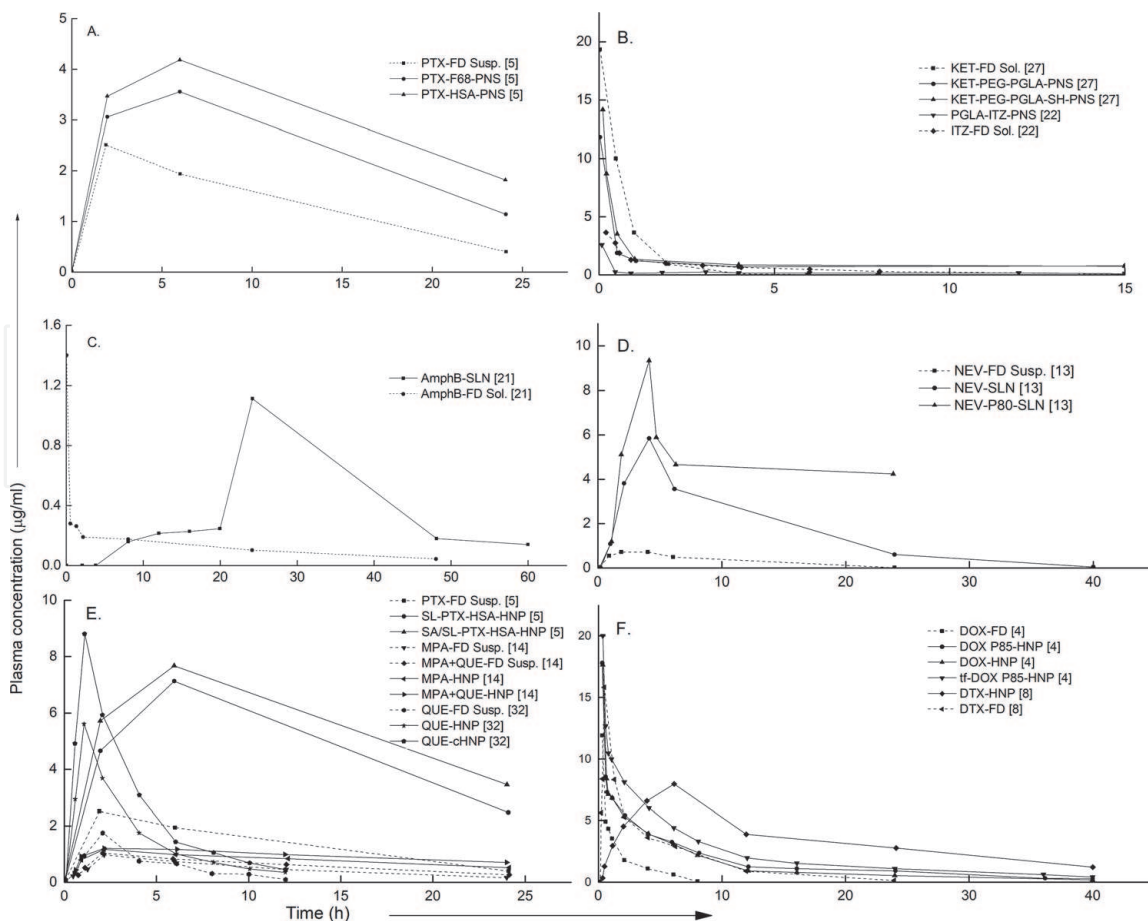
Figure 5.
General behaviors of plasma concentration reported for polymeric nanoparticles (A and B), lipid nanoparticles (C and D), and hybrid nanoparticles (E and F). Oral administration (A, C, and E); intravenous administration (B, D, and F) (PTX: paclitaxel; FD: free drug; F68: Pluronic 68; HSA: human serum albumin; KET: ketamine; SH: shellac; ITZ: itraconazole; NEV: nevirapine; AmphB: amphotericin B; P80: polysorbate 80; SA: stearylamine; SL: soy lecithin; P: PLGA; MPA: mycophenolate; PVA: polyvinyl alcohol; QUE: quercetin; cHNP: cholate-modified hybrid nanoparticle; DOX: doxorubicin; DTX: docetaxel; P85: Pluronic 85; tf: transferrin).

quercetin inhibits the mycophenolate metabolism through cytochrome P450, are highlighted. This, together with the slow-release pattern of the particles, improves in a significant way the *in vivo* performance of the hybrid nanoparticles [14].

Concerning the administration of carriers by the intravenous route, pharmaco-kinetic advantages were also evidenced compared to the free drug administration. As reported by Bian et al. [22] and Han et al. [27], even if a fraction of the polymeric nanoparticles are quickly removed by the reticuloendothelial system during the first 4 h after the administration, the remaining particles into the systemic circulation allow a sustained drug delivery for more than 20 h achieving AUC_{0-t} values from 2 to 10 times higher than free drug. As intended, pegylation of polymeric nanoparticles extends the elimination half-life by ~100 h and increases in 84% the AUC regarding the free drug [27]. With respect to lipid carriers, Lahkar et al. [13] evidence a significant increase of their AUC_{0-t} which could remain in the blood circulation four times more than the free drug. Moreover, modifications to the particle surface providing some hydrophilicity with polysorbate 80 result in an MRT eight times higher than that of the free drug. Regarding the hybrid nanoparticles, Zhu et al. [4] provide evidence on their extended drug delivery pattern that is improved as modifications on the particle surface are introduced. Thus, plasma circulation of the particles and their corresponding AUC_{0-t} could be prolonged up to six and seven times, respectively, compared with that for the free drug. Jadon and Sharma [8] illustrate results in the same direction where drug

delivery from the hybrid particles continues to be detected 72 h after the administration with AUC_{0-t} values around 3.6 times higher than free drug.

4.2 Biodistribution

Figure 6 shows an overview of the organ distribution patterns of the carriers under study as an approximation of their *in vivo* transport and metabolism processes depending on the route of administration. Perhaps, these behaviors would better correspond to the carried drug since the concentration of the active molecule in the tissues of interest is the measure commonly used to follow the particles in this kind of experiments. Once again, it is the intention to illustrate general behaviors; therefore, the punctual analyses on the particular work conditions used by each research team such as the animal models, the sampling times, and the way as the samples were analyzed are not considered. Thus, caution must be taken to do statements that lead to misinterpretations.

As can be seen in **Figure 6**, after 8 h of oral administration of both lipid and hybrid carriers, the liver, the spleen, and the kidney appear as the organs where lipid and hybrid particles are located. This could be attributed to the important role of the liver in the clearance of the particles and the blood filtration function of spleen within the immune system which might also remove the particles of the bloodstream. On its part, drug concentration in the kidney could mean the normal transit of the carrier because of the systemic circulation and the high irrigation of this organ. Nonetheless, the elimination process of intact carriers would also be happening.

On the other hand, as expected, the brain accumulates substantial amounts of lipid nanoparticles administered via intranasal because of the closeness of this organ to the nasal mucosa and its high blood perfusion. This behavior should be harnessed to improve therapies targeted to the brain as those for the treatment of diseases of the central nervous system. Likewise, particles intended for lung cancer therapies, prepared from a hyaluronan-modified polymer, and administered via
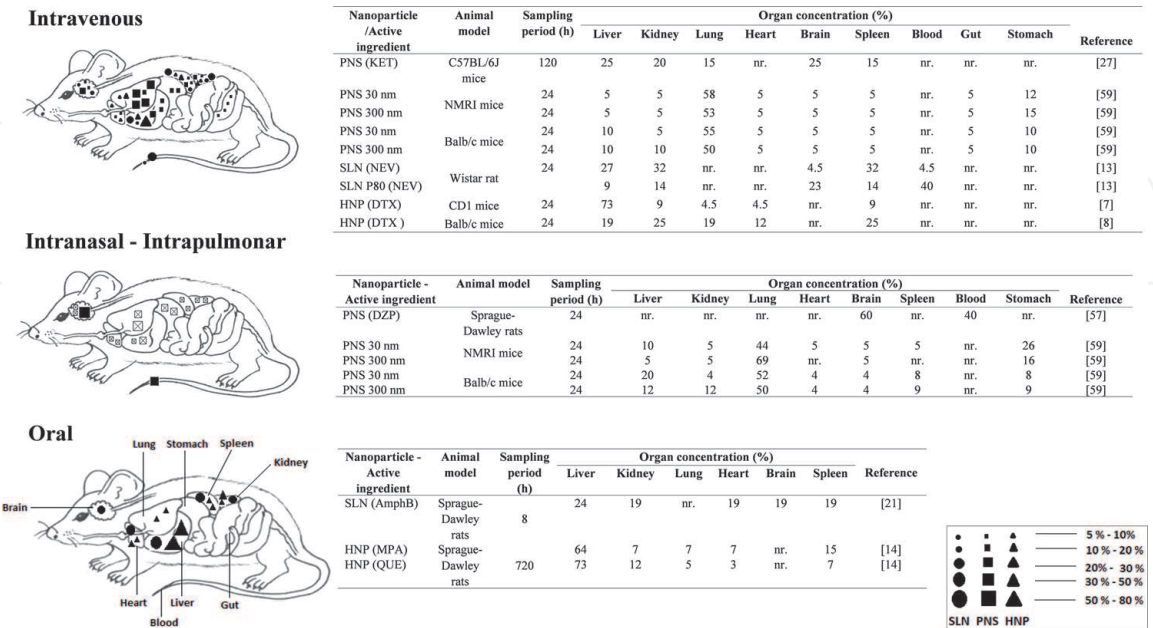
Intravenous

Nanoparticle /Active ingredient	Animal model	Sampling period (h)	Liver	Kidney	Lung	Heart	Brain	Spleen	Blood	Gut	Stomach	Reference
PNS (KET)	C57BL/6J mice	120	25	20	15	nr.	25	15	nr.	nr.	nr.	[27]
PNS 30 nm	NMRI mice	24	5	5	58	5	5	5	nr.	5	12	[59]
PNS 300 nm	NMRI mice	24	5	5	53	5	5	5	nr.	5	15	[59]
PNS 30 nm	Balb/c mice	24	10	5	55	5	5	5	nr.	5	10	[59]
PNS 300 nm	Balb/c mice	24	10	10	50	5	5	5	nr.	5	10	[59]
SLN (NEV)	Wistar rat	24	27	32	nr.	nr.	4.5	32	4.5	nr.	nr.	[13]
SLN P80 (NEV)	Wistar rat	9	14	nr.	nr.	nr.	23	14	40	nr.	nr.	[13]
HNP (DTX)	CD1 mice	24	73	9	4.5	4.5	nr.	9	nr.	nr.	nr.	[7]
HNP (DTX)	Balb/c mice	24	19	25	19	12	nr.	25	nr.	nr.	nr.	[8]

Intranasal - Intrapulmonar

Nanoparticle - Active ingredient	Animal model	Sampling period (h)	Liver	Kidney	Lung	Heart	Brain	Spleen	Blood	Stomach	Reference
PNS (DZP)	Sprague-Dawley rats	24	nr.	nr.	nr.	nr.	60	nr.	40	nr.	[57]
PNS 30 nm	NMRI mice	24	10	5	44	5	5	5	nr.	26	[59]
PNS 300 nm	NMRI mice	24	5	5	69	nr.	5	nr.	nr.	16	[59]
PNS 30 nm	Balb/c mice	24	20	4	52	4	4	8	nr.	8	[59]
PNS 300 nm	Balb/c mice	24	12	12	50	4	4	9	nr.	9	[59]

Oral

Nanoparticle - Active ingredient	Animal model	Sampling period (h)	Liver	Kidney	Lung	Heart	Brain	Spleen	Reference
SLN (AmphB)	Sprague-Dawley rats	8	24	19	nr.	19	19	19	[21]
HNP (MPA)	Sprague-Dawley rats	64	7	7	7	nr.	15		[14]
HNP (QUE)	Sprague-Dawley rats	720	73	12	5	3	nr.	7	[14]

Legend:
- 5 % - 10 %
- 10 % - 20 %
- 20 % - 30 %
- 30 % - 50 %
- 50 % - 80 %

SLN PNS HNP

Figure 6.
General behavior of biodistribution for polymer, lipid, and hybrid nanoparticles after administration by oral, intranasal, intrapulmonary, and intravenous routes. Administration by intravenous, intranasal and oral routes (black-filled symbols) and by intrapulmonary route (crossed symbols) (KET: ketamine; NEV: nevirapine; DTX: docetaxel; DZP: diazepam; AmphB: amphotericin B; MPA: mycophenolate; QUE: quercetin).

intrapulmonary route, directly locate on lung up to 24 h [59]. This finding confirms the ability of hyaluronan to be recognized by cancer lung receptors allowing the particle concentration in this tissue and consequently, avoiding the waste of active substance in other organs.

Regarding the intravenous administration, it seems that after 24 h, polymeric nanoparticles mainly locate at the lung, liver, and brain; lipid particles are distributed in blood, liver, kidney, and spleen; and hybrid particles accumulate in the liver. However, it should be noted that regardless of the kind of particle and compared with the oral and intranasal administration, when carriers are administered by intravenous route, drug is found in low levels in all the investigated organs. In addition, after extended periods (e.g., 120 h), particles are more homogeneously distributed among the investigated tissues [27]. This is a natural consequence of the systemic circulation and the irrigation of the different organs. Besides, as previously mentioned, there is a high probability that the concentration of carriers on the liver occurs due to the ability of the hepatic Kupffer cells to phagocyte them. Likewise, the phagocytic activity of the alveolar macrophages could explain why high concentrations of the drug are found in the lung. In addition, to find carriers or active molecules in the stomach might also be possible considering that the pH of this tissue could favor the retention of active molecules exhibiting a basic nature.

It is important to highlight the efficacy of targeted carriers to reach the intended tissues. As it has been evidenced by Jeannot et al. [59], working with polymeric nanoparticles, the functionalization of the polymer with polysaccharide hyaluronan, known for its affinity toward certain cancer cells receptors, allows high concentrations of particles on the lung offering an interesting alternative for the lung cancer treatment. In the same direction, Dehaini et al. [7] demonstrate the ability of docetaxel-loaded hybrid nanoparticles functionalized with folate to reach cancerous tumors.

4.3 Stability in biological fluids

Knowing if nanoparticles aggregate after their *in vivo* administration is of crucial importance for their application as drug delivery systems. To this end, the colloidal stability of the particulate systems dispersed in biological fluids has been investigated by monitoring variables such as the particle size and the drug encapsulation. Thus, Lazzari et al. [73] demonstrated that polymeric nanospheres prepared by flash nanoprecipitation from PMMA were stable up to 60 h in synthetic saliva, gastric juice, intestinal fluid, and lysosomal fluid while PLA nanoparticles aggregate in gastric juice. Likewise, Dehaini et al. [7] report the aggregation of PLGA nanoparticles in fetal bovine serum (FBS). On the other hand, polymeric nanocapsules coated with brush layers of an oligo ethylene glycol derived methacrylate polymer exhibit major stability in human serum albumin solution, FBS, and human blood plasma, that those non-coated [74]. This evidences the usefulness of designing stealth nanoparticles as a strategy to prevent the particle aggregate formation in blood avoiding their rapid removal from the systemic circulation by the immune system. Regarding SLN, Liu et al. [26] verified their colloidal stability in FBS reporting increases in particle size of approximately 50%, although encapsulation efficiency does not vary. Chaudhari et al. [21] delved into the stability of SLN in simulated gastric fluid confirming that after 2 h, amphotericin B remains encapsulated favoring its stability. With respect to hybrid nanoparticles, contradictory results of aggregation [23] and non-aggregation [7] have been reported when the particle dispersions are mixed with FBS. This can be attributed to the experimental conditions used. In the first case, aggregation is reported after 2 days of storage of the samples at 37°C; in the second one, aggregation was investigated immediately

Nanoparticle	Assay	Experimental conditions				General results	Reference
		Cellular model	**Tracer molecule concentration**	**Interaction— cellular model (some work conditions)**	**Technique of analysis**		
PNS	CD44 expression levels	Human H322, H358, and A549 NSCLC cell lines	8 μg/mL	30 min at 37 C	Flow cytometry FITC	Dose-dependent binding of NP 30 nm and NP 300 nm, was observed in the three cell lines, with a higher intensity for A549 cells compared with H322 and H358 cells.	[59]
HNP	Cellular uptake	The MDA-MB-231 breast cancer cells; human prostate cancer PC3 cells	10, 300, and 500 μg/mL	24 h	CLSM	High internalization of the HNP in the cells at the highest concentrations.	[9]
HNP	Cellular uptake	A549 human lung adenocarcinoma cells	20 μg/mL	24 h	Flow cytometry	Functionalization of HNP plays a key role in the uptake of drugs in *in vitro* lung cancer cells.	[6]
HNP	Cellular uptake Qualitative study	Human breast adenocarcinoma MDA-MB-231 cells	1 μg/mL	12 h	CLSM	The improved cell uptake efficiency of HNP is attributed by cytosolic delivery of the drug.	[8]
HNP	Cellular uptake Quantitative study	Human breast adenocarcinoma MDA-MB-231 cells	Equivalent to 10, 20, 30, and 40 μg/mL	24 h	CLSM	HNP exhibit improved cellular uptake efficiency (45–48%) compared with free drug (37–39%).	[8]
HNP	Cellular uptake analysis	MCF-7 human breast cancer cell	1 μg/mL	2 h	Differential interference contrast microscopy	High internalization of HNP inside the cells after 2 h of incubation with respect to reference nanoparticles.	[14]
HNP	Cellular uptake	Caco-2 cells	25 μg/mL	0.5–2 h	Protein quantification: BCA protein assay kit Drug quantification: HPLC	HNP exhibited improved cellular uptake of quercetin relative to its free form, showing a time-dependent uptake accumulation.	[32]

Nanoparticle	Assay	Experimental conditions				General results	Reference
		Cellular model	Tracer molecule concentration	Interaction—cellular model (some work conditions)	Technique of analysis		
HNP	Internalization into osteoblasts	MC3T3-E1 osteoblasts	2, 4, and 8 μg/mL	6 h at 37°C	CLSM	HNP were more effective in reducing the intracellular MRSA counts than the free linezolid.	[23]
HNP	Cellular internalization	Prostate cancer cells (PC3-MM2) and human breast cancer cells (MDA-MB-231)	100−300 μg/mL	3 min at 37°C	CLSM FITC	Cellular uptake ability depends on particle concentration.	[11]

PNS: polymeric nanospheres; HNP: hybrid nanoparticles; NP: nanoparticle; MTX: methotrexate; FITC: fluorescein isothiocyanate; HPLC: high-performance liquid chromatography; CLSM: confocal laser scanning microscope; MRSA: methicillin-resistant Staphylococcus aureus; *nr.: non-reported data.*

Table 3.
Summary of experimental conditions and general results reported in research works on cellular uptake of nanoparticles prepared by the nanoprecipitation technique.

the particle dispersions were diluted. On the other hand, when the stability of hybrid particles was tested in human plasma, interactions of particle and serum proteins were evidenced which increased the carrier size. But what is more interesting is that those interactions seem to be related to the type of stabilizing agent used. As reported by Godara et al. [5], by using PVA or stearylamine as stabilizing agents, particle sizes increased ~15% that contrast with an increase of ~50% when particles were stabilized with human serum albumin. Maybe, the protein layer covering the particle surfaces promote their interaction with the serum proteins.

4.4 Cellular uptake

Regarding cellular uptake, **Table 3** reports the experimental conditions and general results. Indeed, researches on this regard have been mostly carried out for the hybrid nanoparticles by using human cancer cells taken in their majority from the breast. Nevertheless, some research works have also investigated on prostate and lung cancer cells. Other used cell lines include Caco-2 and MC3T3-E1 osteoblasts. In general terms, the analyses by flow cytometry and confocal laser scanning microscopy reveal that the functionalization of the hybrid particles favors the *in vitro* cellular uptake when compared to the free drugs and the pattern of cellular uptake correlates with the carrier drug loading.

On the other hand, the ability of nanoparticles to penetrate the different physiological barriers and reside in the target tissues has also been demonstrated. For example, SLN could provide efficient *in vivo* skin permeation [26], polymeric nanoparticles might penetrate mucus also exhibiting mucoadhesive behavior [16], and hybrid nanoparticles would cross the enterocyte walls [32] or reach bone tissue [23].

5. Safety and efficacy of carriers prepared by nanoprecipitation

5.1 Safety

A revision of the starting materials used to prepare particles via nanoprecipitation shows that the polymers and lipids present in the different recipes are recognized as safe considering their biocompatibility. Likewise, most organic solvents are classified as with low toxic potential according to ICH [75]. In the cases where acetonitrile, dichloromethane, tetrahydrofuran, dimethylformamide, and even methanol are used as solvents, the obtained particles should meet the specific requirements of limited concentrations of residual solvent because of their inherent toxicity. Traces of organic solvents would remain in the nanoparticle dispersions after the stage of solvent removal during their preparation. For example, up to 2300 ppm of tetrahydrofuran can be detected in lipid nanoparticles, which exceed the limit of 720 ppm established by the ICH [75]. However, as shown in **Table 4**, the safety tests including hematological studies on mice [27], hemolysis assays on human blood [8] or with erythrocytes [5], MTT assay on alveolar epithelial cells [34] or osteoblasts [23], cell viability on cancer cells [9, 11], and histological examination of mice [56], evidence concerns on the safety of that particles, and in general, neither of the particles were prepared via nanoprecipitation. Moreover, nanoparticles reduce the toxicity of the active molecules [8, 57].

5.2 Efficacy

One of the promising applications of nanoparticles, including those obtained by nanoprecipitation, is the therapy against cancer. As shown in **Table 5**, hybrid

Nanoparticle	Experimental conditions for toxicity testing					General results	Reference
	Cellular/animal model	Assay	Drug concentration or dosage used	Time of interaction—cellular model (h)	Technique of analysis		
Polymeric nanoparticles							
PNS	Vero cell line (green monkey kidney epithelial cells)	MTT assay	3.12–100 μg/mL	24 h	ELISA microplate reader	Nanoparticles reduce cytotoxicity of the active molecule.	[57]
PNS	Normal human keratinocytes	MTT assay	0.05 and 0.5 mg/mL	48 h	Microplate reader	No cytotoxic effect was detected after exposure of the NHK for 24 and 48 h to the nanoparticles.	[18]
PNS	Normal human keratinocytes	(H2DCFDA) assay	0.5 mg/mL	1 h	FITC fluorescence	The nanoparticles have no oxidative stress induction potential.	[18]
PNS	Male C57BL/6 J mice	Hematological studies	1 mg/kg	5 days	Hematology analyzer	All hematological parameters assessed at study remained in the normal range for mice.	[27]
Lipid nanoparticles							
SLN	Sprague-Dawley rats	Renal toxicity assessment	3.6 mg/kg	72 h	UV-visible	Freeze-dried nanoparticles are considered as a safe oral alternative.	[21]
SLN	Wistar rats	(OECD) guidelines, 423	5–2000 mg/kg	14 days	LD_{50} by Karber method	None of the animals showed any sign of toxicity. The lethal dose (LD_{50}) of KB is higher than 2000 mg/kg.	[13]
SLN/PNS	BALB/c 3T3	MTT assay	50–200 μM	24 h	Microplate reader	A moderate effect on cell viability, no obvious changes were found.	[26]
Hybrid nanoparticles							
HNP	Normal L929 alveolar epithelial cells	MTT assay	0.1–30 mg/mL	48 h	Spectrophotometric	No significant cytotoxicity against normal alveolar cells.	[34]

Nanoparticle	Experimental conditions for toxicity testing					General results	Reference
	Cellular/animal model	Assay	Drug concentration or dosage used	Time of interaction—cellular model (h)	Technique of analysis		
HNP	MDA-MB-231 breast cancer cells; human prostate cancer PC3 cells; colon cancer HT29 cells	Cell viability	50 to 300 μg/mL	Over night	Fluorescence intensity	No cytotoxic effects were observed for the particles tested.	[9]
HNP	BALB/c female mice	Side effects on vital organs	3 mg/kg	21 days	Histological examination	No significant toxicity to the heart, liver, spleen, lung, or kidney.	[56]
HNP	Whole human blood (from a healthy person)	Hemolysis assay	1 μL of suitably diluted free DTX and HNP	0.5 h	Spectrophotometric	The hemolysis of nanoparticle formulation was lesser than free drug.	[8]
HNP	Sprague-Dawley rats	In vivo toxicity	25 mg/kg	30 days	Spectrophotometric	Concentration of hepatotoxicity biomarkers (ALT and AST) was insignificant as compared to control.	[14]
HNP	MC3T3-E1 osteoblasts	MTT assay	0.5–40 μg/mL	16 h	Microplate reader	All groups showed minimum cytotoxicity against osteoblasts.	[23]
HNP	Erythrocytes	Hemolysis assay	0.7 mg/mL	1 h	Spectrophotometric	The average percentage hemolysis rate of nanoparticles was found between 7 and 16%.	[5]
HNP	Prostate cancer cells (PC3-MM2) and human breast cancer cells (MDA-MB-231)	In vitro cytotoxicity studies	25, 50, 100, 150, 200, and 300 μg/mL	48 h	Measure the luminescence	No cytotoxic effects were observed.	[11]

PNS: polymeric nanospheres; SLN: solid lipid nanoparticles; HNP: hybrid nanoparticles; MTT: 3-(4,5-dimethylthiazol-2-yl)-2,5-diphenyltetrazolium bromide; OECD: Organisation for Economic Co-operation and Development; KB: kokum butter; H2DCFDA: 6-carboxy-2′,7′-dichlorodihydrofluorescein diacetate; NHK: normal human keratinocytes; FITC: fluorescein isothiocyanate; PLGA: poly(D,L-lactide-co-glycolide); ALT: alanine transaminase; AST: aspartate transaminase; DTX: docetaxel; nr.: non-reported data.

Table 4.
Summary of experimental conditions and general results reported in research works on safety testing of nanoparticles prepared by the nanoprecipitation technique.

Nanoparticle	Experimental conditions for efficacy testing					General results	Reference
	Assay	Cellular/animal model	Drug concentration	Time of interaction —cellular model	Technique of analysis		
Polymeric nanoparticles							
PNS (Brazilian red propolis extract)	Antioxidant activity by using DPPH method	—	80 μg/mL	30 min	Spectrophotometry UV	The PNS displayed good antioxidant activity with inhibition values higher than 75%.	[36]
	Antileishmanial *in vitro* assay	L. (V.) braziliensis culture	5–100 μg/mL	24 h	Inverted microscopy	Nanoparticles containing between 30 and 40% of EEP maintained antileishmanial activity like the EEP in its original form.	
PNS (fluticasone propionate)	Mucus mobility by multiple particle tracking	Human cervicovaginal mucus	0.2–0.5 μL (nanosuspension)	30 min	Fluorescent microscopy	Particles exhibit rapid mucus penetration and mucoadhesive behavior.	[16]
	Anti-inflammatory action	Lewi rats	∼0.1 mg of FP/kg	24 h	Total and differential cell counts on an automated cell counter.	Inhibition of bronchoalveolar lavage fluid (BAL) lavage neutrophils between 50 and 70% in 24 h.	
	Duration of residence in mouse lung	CF-1 mouse	10 μg of FP per animal	24 h	HPLC/MS	Upon deposition onto respiratory tissue, solution formulations or non-encapsulated drugs are rapidly removed through absorption into systemic circulation compared with nanoparticles.	
Lipid nanoparticles							
L-βCD-C10 L-βCD-C10/DOPE-PEG L-βCD-C10/ stabilizer (nr.)	Complement protein C3 activation	Polyclonal anti C3 antibody	Topical	75 min	Immuno-electrophoretic	L-βCD-C10/DOPE-PEG shows a low level of complement C3 activation.	[71]

Nanoparticle	Experimental conditions for efficacy testing					General results	Reference
	Assay	Cellular/animal model	Drug concentration	Time of interaction —cellular model	Technique of analysis		
SLN/PNS (tetracaine)	Franz diffusion cell	Hairless abdominal full-thickness skins of Sprague-Dawley rats	Corresponding to 5 mg of tetracaine	72 h	Spectrophotometry UV	SLN provides an efficient *in vitro* permeation and sustained performance up to 72 h.	[26]
	Tail-flick test	Sprague-Dawley rats	0.25 mg/mL	4 h	Response threshold (seconds to withdraw the tail before the thermal stimulus).	PNS exhibited prolonged antinociceptive effect showing efficiency until 3.5 h of study.	
	Paw pressure test	Sprague-Dawley rats	0.25 mg/mL	8 h	Response threshold (amount of pressure supported by the animal before removing the paw).	The analgesic effects are maintained for a longer period. Greater than 50% pain control was still found at 6 and 4 h for PNS and SLN, respectively.	
SLN (polymyxin B)	Antimicrobial evaluation	Strain of *E. coli*	6.6 μg/mL	2–18 h	Turbidimetry	Activity (% inhibition of growth) by the plain drug and SLN were 52.7 and 56.7%, respectively.	[20]
SLN (amphotericin B)	*In vitro* antifungal efficacy	*C. albicans*	0.5–250 μg/mL	48 h	Change in original blue color of resazurin to pink.	Minimum inhibitory concentration value of 7.812 μg/mL attributed to controlled release of drug from the nanoparticulate matrix.	[21]
Hybrid nanoparticles							
HNP (docetaxel)	Targeting studies	KB cells	0.25 mg/mL	30 min	Flow cytometry	The targeted hybrid nanoparticles were found much deeper within the tumor and further away from the vasculature.	[7]
	In vivo tumor treatment efficacy	Female nude mice	4 mg/kg	35 days	Tumor width, length, and size	Half of the mice were still alive at 64 days after tumor challenge. As an indicator of global health, body weights were monitored over the course of the study.	

Nanoparticle	Experimental conditions for efficacy testing					General results	Reference
	Assay	Cellular/animal model	Drug concentration	Time of interaction —cellular model	Technique of analysis		
HNP (methotrexate)	Antiproliferation assay	MDB-MB-231 breast cancer and PC3 prostate cancer cells	5, 10, 20, 50, 100, 150, and 200 µg/mL	72 h	ATP-based cell viability kit	MTX encapsulated in the HNP preserve its anticancer activity.	[9]
HNP (doxorubicin)	Cytotoxicity evaluation	HL-60 cells and HL-60/ DOX. MTT assay	0.25, 0.5, 1, 2, 5, 10, and 20 µg/mL	70 h	Microplate reader	The cytotoxicity activity of HNP was superior to DOX solution. The IC$_{50}$ of HNP was lower than DOX solution.	[4]
	Tumor growth inhibition	Male BALB/c mice	20 mg/kg	18 days	Xenograft model	The tumor growth inhibition was (68.9–89.6%). The body weight of the mice in any of HNP treatments groups showed no obvious decrease in comparison with untreated groups.	
HNP (paclitaxel)	Cytotoxicity (MTT assay)	A549 human lung adenocarcinoma cells	0.5–10 mg/mL	48 h	Microplate reader	Drugs loaded HNP exhibited marked cytotoxicity on cells in a dose-dependent way and showed higher cytotoxicity compared with their free drug counterparts.	[6]
	Synergistic effects	A549 human lung adenocarcinoma cells	0.5–10 mg/mL	48 h	The results of cytotoxicity were evaluated via the Combination Index	The *in vivo* and *in vitro* results show synergetic effect of the two drugs incorporated in HNP against the lung cancer.	
	In vivo antitumor efficacy	BALB/c-nude mice	5 mg/kg of paclitaxel and 3 mg/kg of triptolide	18 days	Tumor width, length, and size	The inhibition of the *in vivo* tumor growth was lesser than that of the control group.	

Nanoparticle	Experimental conditions for efficacy testing					General results	Reference
	Assay	Cellular/animal model	Drug concentration	Time of interaction —cellular model	Technique of analysis		
HNP (psoralen)	Antitumor efficacy	MCF-7 cells	3 mg/kg	21 days	Changes in the tumor volume and final tumor weight	HNP show more efficient antitumor effects respect to other formulations.	[56]
HNP (docetaxel)	Cytotoxicity (MTT assay)	Human breast adenocarcinoma MDA-MB-231 cells	0.05, 0.1, 1, 10, and 20 μg/mL	24, 48, and 72 h	ELISA plate reader	Cytotoxicity activity of HNP could be attributed to lipid-mediated cytosolic delivery of the drug which is dose dependent.	[8]
	Annexin V-FITC/ propidium iodide apoptosis assay	MDA-MB-231 cells	10 μg/mL	24 h	Flow cytometry	Injured cells (including early apoptosis, late apoptosis, and necrotic cells) with HNP are greater (87%) as compared with free drug (51%).	
	Antitumor efficiency	BALB/c female mice	10 mg/kg	3 weeks	Tumor width, length and size	The repeated dosing of HNP exhibit less mortality (33%) than with free drug.	
HNP (mycophenolate; quercetin)	Annexin V apoptosis assay	MCF-7	10, 20, 40, and 60 μg/mL	6 h	CLSM	Apoptosis indices of MPA-NP and QC-NP are higher compared to respective free drugs. Moreover, the apoptosis index is significantly higher when combination MPA-NP + QC-NP is used.	[14]
	Inosine-5′-monophosphate dehydrogenase (IMPDH) assay	MCF-7	1 μM MPA NP	24 h	IMPDH assay kit	Significantly higher enzyme inhibition was observed in MPA-NP than free MPA.	

Nanoparticle	Experimental conditions for efficacy testing					General results	Reference
	Assay	Cellular/animal model	Drug concentration	Time of interaction —cellular model	Technique of analysis		
	In vivo antitumor efficacy	Sprague-Dawley rats	25 mg/kg	30 days	Tumor width, length, and size	Combination therapy of MPA and QC loaded LPN demonstrates significant suppression of tumor growth as compared to other groups.	
	Cytotoxicity (MTT assay)	MCF-7 human breast cancer cell	10, 20, 40, and 60 μg/mL	nr.	Optical density	Combination treatment of nanoparticles (MPA-NP + QC-NP) shows significantly higher cytotoxic effect compared with individual nanopreparation (MPA-NP and QC-NP).	
HNP (quercetin)	Cellular internalization	Caco-2 cells	25 mg/kg	0.5 h	CLSM	Excellent affinity and permeability to enterocytes allows HNP to be efficiently transported.	[32]
	Cytotoxic evaluation on P388 cells (MTT assay)	Lymphoblastic leukemia P388 cells	5, 10, and 20 μM	24 h	Spectrophotometry UV	HNP have higher cellular approachability that accords well with the cellular uptake by Caco-2 cells.	
	In vivo antileukemic effect	DBA/2 mice	25 mg/kg	21 days	Automatic blood counter	HNP can enhance the oral bioavailability of QC.	
HNP (paclitaxel)	Plasma protein binding study	Blood sample from a healthy volunteer	0.7 mg/mL	2 h	Bradford assay	The protein binding of HNP was found between 15.1 and 33.7%. The interaction between the biological environment and HNP can be controlled by surfactant.	[5]

Nanoparticle	Experimental conditions for efficacy testing					General results	Reference
	Assay	Cellular/animal model	Drug concentration	Time of interaction —cellular model	Technique of analysis		
HNP (linezolid)	Minimum inhibitory concentration (MIC)	Strains of USA300-0114, CDC-587, and RP-62A	500 µg/mL stock solution in TSB, and serially diluted for the assay	24 h	Broth dilution method Microplate reader	The MIC50 and MIC90 values of free linezolid were approximately 40–50% of the values of HNP.	[23]
	Biofilm microplate assay	*S. aureus*	32, 64, 128, 164, and 256 µg/mL	12 h	Microplate reader	HNP were more effective than free linezolid for eradicating the MRSA biofilm.	
	Biofilm microplate assay	*S. aureus*	32, 64, 128, 164, and 256 µg/mL	12 h	CLSM	Extensive retention of the nanoparticles in the biofilms even after multiple buffer washing.	
	Drug's levels in animals' bones	Sprague-Dawley rats	32, 64, 128, 164, and 256 µg/mL	24 h	HPLC	Bone linezolid levels from HNP increase to over four-folds those of the free drug.	
HNP (sorafenib)	Cell growth inhibition assay	Prostate cancer cells (PC3-MM2) and human breast cancer cells (MDA-MB-231)	5, 10, 20, 50, 100, 150, and 200 µg/mL	72 h	Cell viability kit	The inhibition of the tumor cell growth was found to be time- and dose dependent for drug solution as well as HNP.	[11]

PNS: polymeric nanospheres; SLN: solid lipid nanoparticles; NLC: nanostructured lipid carriers; HNP: hybrid nanoparticles; CD: cyclodextrin; IC50: half-maximal inhibitory concentration; MPA: mycophenolate; Nv: nevirapine; QC: quercetin; MIC: minimum inhibitory concentration; MTS: 3-(4,5-dimethylthiazol-2-yl)-5-(3-carboxymethoxyphenyl)-2-(4-sulfophenyl)-2H-tetrazolium; LRP: luciferase reporter phage; CFU: colony-forming units; MTT: 3-(4,5-dimethylthiazol-2-yl)-2,5-diphenyltetrazolium bromide; DOX: doxorubicin; MTX: methotrexate; HL-60: human leukemia cell line; DPPH: 2,2-diphenyl-1-picryhydrazyl; EEP: ethanolic extract of propolis; NSCLCs: non-small cell lung cancers; NMRI: Naval Medical Research Institute; MS: mass spectrometer; HPLC: high-performance liquid chromatography; CLSM: confocal laser scanning microscopy, nr.: non-reported data.

Table 5.
Summary of experimental conditions and general results reported in research works on efficacy testing of nanoparticles prepared by the nanoprecipitation technique.

nanoparticles give good results in this sense. First, the incorporation of the active molecules into the carriers preserve the anticancer activity [9] and nanoparticles offer better performance compared with the free drug [4, 14, 56], in some cases being dose dependent [6, 8, 11]. Besides, significant improvements in the *in vivo* anticancer performance were achieved by the encapsulation of both an anticancer molecule (mycophenolate) and an antioxidant agent (quercetin) into the same hybrid nanoparticle, as quercetin prevents mycophenolate of its hepatic metabolism via the oxygenase enzymes [14]. Moreover, it was demonstrated that the *in vivo* tumor treatment in mice prolongs the life of the animals [7].

Taken advantage of the slow-release patterns that could be obtained with nanoparticulated systems, the development of carriers exhibiting antimicrobial and anesthetic activities are also of interest in research. Thus, the lowest values of minimum inhibitory concentrations of SLN containing polymyxin B or amphotericin B [20, 21] with respect to the free drugs contribute to support the applicability of nanoparticles prepared by nanoprecipitation in this area. In line with this, polymeric nanoparticles containing Brazilian red propolis extract have also shown antileishmanial activity [36], and linezolid-loaded hybrid nanoparticles demonstrated their ability to be retained in biofilms optimizing their antibacterial performance [23]. Regarding the behavior of nanoparticles in anesthetic and anti-inflammatory tests, tetracaine-loaded SLN exhibited prolonged antinociceptive effect leading to better control of pain [26].

Finally, the possibilities to get target particles prepared by the nanoprecipitation technique have been opened from the research works of Jeannot et al. [59] and Dehaini et al. [7] who investigate hyaluronan and folate as receptors chemically bonded to the polymer obtaining promising results for cancer therapies.

6. Conclusions

Nanoprecipitation is a simple, energy-efficient, and versatile method to entrap active molecules into carriers at the submicron and nanometric levels being the most common developments those oriented to obtain polymer, lipid, and hybrid particles. As the knowledge on the *in vivo* behavior of nanocarriers progresses and the need to produce them at the industrial scale demands for greater efficiency, the technique and the used starting materials have been optimized to improve the characteristics of the carriers and the control and standardization of continuous processes. In this way, sophisticated devices have been proposed to get sizes lower than 100 nm and the procedure has been refined, either through the chemical modification of polymers or through the careful definition of the work conditions, leading to particles entrapping hydrophobic and hydrophilic molecules, or exhibiting a targeted performance, a positive charge on their surface, or behaviors as stealth carriers. Moreover, the hybrid nanoparticles are promising drug delivery systems where the advantages of both polymeric and lipid particles are harnessed in their design to offer major drug loadings, slow drug-release patterns, and better pharmacokinetic properties. Regardless of the type of carrier, nanoprecipitation seems to be appropriate to obtain safe particles. Even using solvents characterized by inherent toxicity, the satisfactory results achieved by safety tests support their applicability in pharmaceutics. On this basis, it is expected that research on nanoprecipitation will continue looking for innovative solutions to the challenges facing current and future medicine. Some of the findings reported by different research teams and summarized in this chapter provide valuable insights regarding the potentialities of this technique in this respect.

Author details

Oscar Iván Martínez-Muñoz, Luis Fernando Ospina-Giraldo
and Claudia Elizabeth Mora-Huertas*
Departamento de Farmacia, Facultad de Ciencias, Universidad Nacional de
Colombia Sede Bogotá, Bogotá, Colombia

*Address all correspondence to: cemorah@unal.edu.co

IntechOpen

References

[1] Fessi H, Puisieux F, Devissaguet JP. Procédé de préparation de systèmes colloïdaux dispersibles d'une substance sous forme de nanocapsules. European Patent 1988;274961 A1, 20 July

[2] Fessi H, Puisieux F, Devissaguet JP, Ammoury N, Benita S. Nanocapsule formation by interfacial polymer deposition following solvent displacement. International Journal of Pharmaceutics. 1989;**55**:R1-R4. DOI: 10.1016/0378-5173(89)90281-0

[3] Schubert S, Delaney JT, Schubert US. Nanoprecipitation and nanoformulation of polymers: From history to powerful possibilities beyond poly (lactic acid). Soft Matter. 2011;**7**:1581-1588. DOI: 10.1039/c0sm00862a

[4] Zhu B, Zhang H, Yu L. Novel transferrin modified and doxorubicin loaded Pluronic 85/lipid-polymeric nanoparticles for the treatment of leukemia: In vitro and in vivo therapeutic effect evaluation. Biomedicine & Pharmacotherapy. 2017;**86**:547-554. DOI: 10.1016/j.biopha.2016.11.121

[5] Godara S, Lather V, Kirthanashri VS, Awasthi R, Pandita D. Lipid-PLGA hybrid nanoparticles of paclitaxel: Preparation, characterization, in vitro and in vivo evaluation. Materials Science and Engineering C. 2020;**109**: 110576. DOI: 10.1016/j.msec.2019.110576

[6] Liu J, Cheng H, Han L, Qiang Z, Zhang X, Gao W, et al. Synergistic combination therapy of lung cancer using paclitaxel- and triptolide-coloaded lipid–polymer hybrid nanoparticles. Drug Design, Development and Therapy. 2018;**12**:3199-3209. DOI: 10.2147/dddt.s172199

[7] Dehaini D, Fang RH, Luk BT, Pang Z, Hu CMJ, Kroll AV, et al. Ultra-small lipid–polymer hybrid nanoparticles for tumor-penetrating drug delivery. Nanoscale. 2016;**8**:14411-14419. DOI: 10.1039/c6nr04091h

[8] Jadon RS, Sharma M. Docetaxel-loaded lipid-polymer hybrid nanoparticles for breast cancer therapeutics. Journal of Drug Delivery Science and Technology. 2019;**51**: 475-484. DOI: 10.1016/j.jddst.2019.03.039

[9] Tahir N, Madni A, Balasubramanian V, Rehman M, Correia A, Kashif PM, et al. Development and optimization of methotrexate-loaded lipid-polymer hybrid nanoparticles for controlled drug delivery applications. International Journal of Pharmaceutics. 2017;**533**:156-168. DOI: 10.1016/j.ijpharm.2017.09.061

[10] Alshamsan A. Nanoprecipitation is more efficient than emulsion solvent evaporation method to encapsulate cucurbitacin I in PLGA nanoparticles. Saudi Pharmaceutical Journal. 2014;**22**: 219-222. DOI: 10.1016/j.jsps.2013.12.002

[11] Tahir N, Madni A, Li W, Correia A, Khan MM, Rahim MA, et al. Microfluidic fabrication and characterization of sorafenib-loaded lipid-polymer hybrid nanoparticles for controlled drug delivery. International Journal of Pharmaceutics. 2020;**581**:119275. DOI: 10.1016/j.ijpharm.2020.119275

[12] Raina H, Kaur S, Jindal AB. Development of efavirenz loaded solid lipid nanoparticles: Risk assessment, quality-by-design (QbD) based optimisation and physicochemical characterisation. Journal of Drug Delivery Science and Technology. 2017;**39**:180-191. DOI: 10.1016/j.jddst.2017.02.013

[13] Lahkar S, Das MK. Surface modified kokum butter lipid nanoparticles for the brain targeted delivery of nevirapine.

Journal of Microencapsulation. 2018;**35**: 680-694. DOI: 10.1080/ 02652048.2019.1573857

[14] Patel G, Thakur NS, Kushwah V, Patil MD, Nile SH, Jain S, et al. Mycophenolate co-administration with quercetin via lipid-polymer hybrid nanoparticles for enhanced breast cancer management. Nanomedicine: Nanotechnology, Biology and Medicine. 2020;**24**:102147. DOI: 10.1016/j. nano.2019.102147

[15] Hu FQ, Jiang SP, Du YZ, Yuan H, Ye YQ, Zeng S. Preparation and characteristics of monostearin nanostructured lipid carriers. International Journal of Pharmaceutics. 2006;**314**:83-89. DOI: 10.1016/j. ijpharma.2006.01.040

[16] Popov A, Schopf L, Bourassa J, Chen HB. Enhanced pulmonary delivery of fluticasone propionate in rodents by mucus-penetrating nanoparticles. International Journal of Pharmaceutics. 2016;**502**:188-197. DOI: 10.1016/j. ijpharm.2016.02.031

[17] Albisa A, Piacentini E, Sebastian V, Arruebo M, Santamaria J, Giorno L. Preparation of drug-loaded PLGA-PEG nanoparticles by membrane-assisted nanoprecipitation. Pharmaceutical Research. 2017;**34**:1296-1308. DOI: 10.1007/s11095-017-2146-y

[18] Sahle FF, Gerecke C, Kleuser B, Bodmeier R. Formulation and comparative in vitro evaluation of various dexamethasone-loaded pH-sensitive polymeric nanoparticles intended for dermal applications. International Journal of Pharmaceutics. 2017;**516**:21-31. DOI: 10.1016/j. ijpharm.2016.11.029

[19] Mora-Huertas CE, Garrigues O, Fessi H, Elaissari A. Nanocapsules prepared via nanoprecipitation and emulsification-diffusion methods: Comparative study. European Journal of

Pharmaceutics and Biopharmaceutics. 2012;**80**:235-239. DOI: 10.1016/j. ejpb.2011.09.013

[20] Pattani AS, Mandawgade SD, Patravale VB. Development and comparative anti-microbial evaluation of lipid nanoparticles and nanoemulsion of polymyxin B. Journal of Nanoscience and Nanotechnology. 2006;**6**: 2986-2990. DOI: 10.1166/jnn.2006.459

[21] Chaudhari MB, Desai PP, Patel PA, Patravale VB. Solid lipid nanoparticles of amphotericin B (AmbiOnp): In vitro and in vivo assessment towards safe and effective oral treatment module. Drug Delivery and Translational Research. 2016;**6**:354-364. DOI: 10.1007/ s13346-015-0267-6

[22] Bian X, Liang S, John J, Hsiao CH, Wei X, Liang D, et al. Development of PLGA-based itraconazole injectable nanospheres for sustained release. International Journal of Nanomedicine. 2013;**8**:4521-4531. DOI: 10.2147/IJN. S54040

[23] Guo P, Buttaro BA, Xue HY, Tran NT, Wong HL. Lipid-polymer hybrid nanoparticles carrying linezolid improve treatment of methicillin-resistant *Staphylococcus aureus* (MRSA) harbored inside bone cells and biofilms. European Journal of Pharmaceutics and Biopharmaceutics. 2020;**151**:189-198. DOI: 10.1016/j.ejpb.2020.04.010

[24] Dong Y, Ng WK, Shen S, Kim S, Tan RBH. Solid lipid nanoparticles: Continuous and potential large-scale nanoprecipitation production in static mixers. Colloids and Surfaces B: Biointerfaces. 2012;**94**:68-72. DOI: 10.1016/j.colsurfb.2012.01.018

[25] Torres-Flores G, Nazende GT, Emre TA. Preparation of fenofibrate loaded Eudragit L100 nanoparticles by nanoprecipitation method. Materials Today: Proceedings. 2019;**13**:428-435. DOI: 10.1016/j.matpr.2019.03.176

[26] Liu X, Zhao Q. Long-term anesthetic analgesic effects: Comparison of tetracaine loaded polymeric nanoparticles, solid lipid nanoparticles, and nanostructured lipid carriers in vitro and in vivo. Biomedicine & Pharmacotherapy. 2019;**117**:109057. DOI: 10.1016/j.biopha.2019.109057

[27] Han FY, Liu Y, Kumar V, Xu W, Yang G, Zhao CX, et al. Sustained-release ketamine-loaded nanoparticles fabricated by sequential nanoprecipitation. International Journal of Pharmaceutics. 2020;**581**:119291. DOI: 10.1016/j.ijpharm.2020.119291

[28] Hu FQ, Zhang Y, Du YZ, Yuan H. Nimodipine loaded lipid nanospheres prepared by solvent diffusion method in a drug saturated aqueous system. International Journal of Pharmaceutics. 2008;**348**:146-152. DOI: 10.1016/j.ijpharma.2007.07.025

[29] Chourasiya V, Bohrey S, Pandey A. Formulation, optimization, characterization and in-vitro drug release kinetics of atenolol loaded PLGA nanoparticles using 33 factorial design for oral delivery. Materials Discovery. 2016;**5**:1-13. DOI: 10.1016/j.md.2016.12.002

[30] Oliveira DRB, Furtado GF, Cunha RL. Solid lipid nanoparticles stabilized by sodium caseinate and lactoferrin. Food Hydrocolloids. 2019;**90**:321-329. DOI: 10.1016/j.foodhyd.2018.12.025

[31] Khayata N, Abdelwahed W, Chehnaa MF, Charcosset C, Fessi H. Preparation of vitamin E loaded nanocapsules by the nanoprecipitation method: From laboratory scale to large scale using a membrane contactor. International Journal of Pharmaceutics. 2012;**423**:419-427. DOI: 10.1016/j.ijpharma.2011.12.016

[32] Lee MK, Lim SJ, Kim CK. Preparation, characterization and in vitro cytotoxicity of paclitaxel-loaded sterically stabilized solid lipid nanoparticles. Biomaterials. 2007;**28**:2137-2146. DOI: 10.1016/j.biomaterials.2007.01.014

[33] Miladi K, Sfar S, Fessi H, Elaissari A. Encapsulation of alendronate sodium by nanoprecipitation and double emulsion: From preparation to in vitro studies. Industrial Crops and Products. 2015;**72**:24-33. DOI: 10.1016/j.indcrop.2015.01.079

[34] Ahmaditabar P, Momtazi-Borojeni AA, Rezayan AH, Mahmoodi M, Sahebkar A, Mellat M. Enhanced entrapment and improved in vitro controlled release of N-acetyl cysteine in hybrid PLGA/lecithin nanoparticles prepared using a nanoprecipitation/self-assembly method. Journal of Cellular Biochemistry. 2017;**118**:4203-4209. DOI: 10.1002/jcb.26070

[35] Allen S, Osorio O, Liu YG, Scott E. Facile assembly and loading of theranostic polymersomes via multi-impingement flash nanoprecipitation. Journal of Controlled Release. 2017;**262**:91-103. DOI: 10.1016/j.jconrel.2017.07.026

[36] Do Nascimento TG, Da Silva PF, Azevedo LF, Da Rocha LG, Porto ICCM, Moura TFAL, et al. Polymeric nanoparticles of Brazilian red propolis extract: Preparation, characterization, antioxidant and leishmanicidal activity. Nanoscale Research Letters. 2016;**11**:301. DOI: 10.1186/s11671-016-1517-3

[37] Lammari N, Louaer O, Meniai AH, Elaissari A. Encapsulation of essential oils via nanoprecipitation process: Overview, progress, challenges and prospects. Pharmaceutics. 2020;**12**:431. DOI: 10.3390/pharmaceutics12050431

[38] Mora-Huertas CE, Fessi H, Elaissari A. Polymer-based nanocapsules for drug delivery. International Journal of Pharmaceutics. 2010;**385**:113-142. DOI: 10.1016/j.ijpharm.2009.10.018

[39] Arizaga A, Ibarz G, Piñol R, Urtizberea A. Encapsulation of magnetic nanoparticles in a pH-sensitive poly (4-vinyl pyridine) polymer: A step forward to a multi-responsive system. Journal of Experimental Nanoscience. 2014;**9**: 561-569. DOI: 10.1080/17458080.2012.678393

[40] Villela AL, Martynek D, Bautkinová T, Šoó M, Ulbrich P, Raquez J-M, et al. Self-assembly of poly(L-lactide-co-glycolide) and magnetic nanoparticles into nanoclusters for controlled drug delivery. European Polymer Journal. 2020;**133**:109795. DOI: 10.1016/j.eurpolymj.2020.109795

[41] Fan Y, Yuan S, Huo MM, Chaudhuri AS, Zhao M, Wu Z, et al. Spatial controlled multistage nanocarriers through hybridization of dendrimers and gelatin nanoparticles for deep penetration and therapy into tumor tissue. Nanomedicine: Nanotechnology, Biology and Medicine. 2017;**13**:1399-1410. DOI: 10.1016/j.nano.2017.01.008

[42] Charcosset C, El-Harati A, Fessi H. Preparation of solid lipid nanoparticles using a membrane contactor. Journal of Controlled Release. 2005;**108**:112-120. DOI: 10.1016/j.jconrel.2005.07.023

[43] D'oria C, Charcosset C, Barresi AA, Fessi H. Preparation of solid lipid particles by membrane emulsification-influence of process parameters. Colloids and Surfaces A: Physicochemical and Engineering Aspects. 2009;**338**:114-118. DOI: 10.1016/j.colsurfa.2009.01.003

[44] Valente I, Celasco E, Marchisio DL, Barresi AA. Nanoprecipitation in confined impinging jets mixers: Production, characterization and scale-up of pegylated nanospheres and nanocapsules for pharmaceutical use. Chemical Engineering Science. 2012;**77**:217-227. DOI: 10.1016/j.ces.2012.02.050

[45] Tao J, Chow SF, Zheng Y. Application of flash nanoprecipitation to fabricate poorly water-soluble drug nanoparticles. Acta Pharmaceutica Sinica B. 2019;**9**:4-18. DOI: 10.1016/j.apsb.2018.11.001

[46] Martínez Rivas CJ, Tarhini M, Badri W, Miladi K, Greige-Gerges H, Nazari QA, et al. Nanoprecipitation process: From encapsulation to drug delivery. International Journal of Pharmaceutics. 2017;**532**:66-81. DOI: 10.1016/j.ijpharm.2017.08.064

[47] Mora-Huertas CE, Fessi H, Elaissari A. Influence of process and formulation parameters on the formation of submicron particles by solvent displacement and emulsification-diffusion methods. Advances in Colloid and Interface Science. 2011;**163**:90-122. DOI: 10.1016/j.cis.2011.02.005

[48] Saad WS, Prud'homme RK. Principles of nanoparticle formation by flash nanoprecipitation. Nano Today. 2016;**11**:212-227. DOI: 10.1016/j.nantod.2016.04.006

[49] Couvreur P, Stella B, Reddy LH, Hillaireau H, Dubernet C, Desmaële D, et al. Squalenoyl nanomedicines as potential therapeutics. Nano Letters. 2006;**6**:2544-2548. DOI: 10.1021/nl061942q

[50] Stainmesse S, Orecchioni AM, Nakache E, Puisieux F, Fessi H. Formation and stabilization of a biodegradable polymeric colloidal suspension of nanoparticles. Colloid & Polymer Science. 1995;**273**:505-511. DOI: 10.1007/BF00656896

[51] Quintanar-Guerrero D, Allémann E, Fessi H, Doelker E. Preparation techniques and mechanisms of formation of biodegradable nanoparticles from preformed polymers. Drug Development and Industrial Pharmacy. 1998;**24**(12):

1113-1128. DOI: 10.3109/
03639049809108571

[52] François G, Katz JL. Nanoparticles and nanocapsules created using the ouzo effect: Spontaneous emulsification as an alternative to ultrasonic and high-shear devices. ChemPhysChem. 2005;**6**:209-216. DOI: 10.1002/cphc.200400527

[53] Lepeltier E, Bourgaux C, Couvreur P. Nanoprecipitation and the "ouzo effect": Application to drug delivery devices. Advanced Drug Delivery Reviews. 2014;**71**:86-97. DOI: 10.1016/j.addr.2013.12.009

[54] Martínez-Acevedo L, Zambrano-Zaragoza M, Vidal-Romero G, Mendoza-Elvira S, Quintanar-Guerrrero D. Evaluation of the lubricating effect of magnesium stearate and glyceryl behenate solid lipid nanoparticles in a direct compression process. International Journal of Pharmaceutics. 2018;**545**:170-175. DOI: 10.1016/j.ijpharm.2018.05.002

[55] Noriega-Pelaez EK, Mendoza-Muñoz N, Ganem-Quintanar A, Quintanar-Guerrero D. Optimization of the emulsification and solvent displacement method for the preparation of solid lipid nanoparticles. Drug Development and Industrial Pharmacy. 2011;**37**:160-166. DOI: 10.3109/03639045.2010.50180

[56] Du M, Ouyang Y, Meng F, Zhang X, Ma Q, Zhuang Y, et al. Polymer-lipid hybrid nanoparticles: A novel drug delivery system for enhancing the activity of Psoralen against breast cancer. International Journal of Pharmaceutics. 2019;**561**:274-282. DOI: 10.1016/j.ijpharm.2019.03.006

[57] Sharma D, Sharma RK, Sharma N, Gabrani R, Sharma SK, Ali J, et al. Nose-to-brain delivery of PLGA-diazepam nanoparticles. American Association of Pharmaceutical Scientists. 2015;**16**:

1108-1121. DOI: 10.1208/s12249-015-0294-0

[58] Jenning V, Thünemann AF, Gohla SH. Characterisation of a novel solid lipid nanoparticle carrier system based on binary mixtures of liquid and solid lipids. International Journal of Pharmaceutics. 2000;**199**:167-177. DOI: 10.1016/S0378-5173(00)00378-1

[59] Jeannot V, Mazzaferro S, Lavaud J, Laetitia V, Henry M, Arboléas M, et al. Targeting CD44 receptor-positive lung tumors using polysaccharide-based nanocarriers: Influence of nanoparticle size and administration rout. Nanomedicine: Nanotechnology, Biology and Medicine. 2015;**12**:921-932. DOI: 10.1016/j.nano.2015.11.018

[60] Tahara K, Karasawa K, Onodera R, Takeuchi H. Feasibility of drug delivery to the eye's posterior segment by topical instillation of PLGA nanoparticles. Asian Journal of Pharmaceutical Sciences. 2017;**12**:394-399. DOI: 10.1016/j.ajps.2017.03.002

[61] Zhao J, Stenzel MH. Entry of nanoparticles into cells: The importance of nanoparticle properties. Polymer Chemistry. 2018;**9**:259-273. DOI: 10.1039/C7PY01603D

[62] Yin J, Hou Y, Song X, Wang P, Li Y. Cholate-modified polymer-lipid hybrid nanoparticles for oral delivery of quercetin to potentiate the antileukemic effect. International Journal of Nanomedicine. 2019;**14**:4045-4057. DOI: 10.2147/ijn.s210057

[63] Helgason T, Awad TS, Kristbergsson K, McClements DJ, Weiss J. Effect of surfactant surface coverage on formation of solid lipid nanoparticles (SLN). Journal of Colloid and Interface Science. 2009;**334**:75-81. DOI: 10.1016/j.jcis.2009.03.012

[64] Bunjes H, Drechsler M, Koch MHJ, Westesen K. Incorporation of the model

drug ubidecarenone into solid lipid nanoparticles. Pharmaceutical Research. 2001;**18**:287-293. DOI: 10.1023/A: 1011042627714

[65] Jores K, Mehnert W, Drechsler M, Bunjes H, Johann C, Mäder K. Investigations on the structure of solid lipid nanoparticles (SLN) and oil-loaded solid lipid nanoparticles by photon correlation spectroscopy, field-flow fractionation and transmission electron microscopy. Journal of Controlled Release. 2004;**95**:217-227. DOI: 10.1016/ j.jconrel.2003.11.012

[66] Gordillo-Galeano A, Mora-Huertas CE. Solid lipid nanoparticles and nanostructured lipid carriers: A review emphasizing on particle structure and drug release. European Journal of Pharmaceutics and Biopharmaceutics. 2018;**133**:285-308. DOI: 10.1016/j. ejpb.2018.10.017

[67] Westesen K, Bunjes H, Koch MHJ. Physicochemical characterization of lipid nanoparticles and evaluation of their drug loading capacity and sustained release potential. Journal of Controlled Release. 1997;**48**:223-236. DOI: 10.1016/S0168-3659(97)00046-1

[68] Pardeike J, Hommoss A, Müller RH. Lipid nanoparticles (SLN, NLC) in cosmetic and pharmaceutical dermal products. International Journal of Pharmaceutics. 2009;**366**:170-184. DOI: 10.1016/j.ijpharm.2008.10.003

[69] Weber S, Zimmer A, Pardeike J. Solid lipid nanoparticles (SLN) and nanostructured lipid carriers (NLC) for pulmonary application: A review of the state of the art. European Journal of Pharmaceutics and Biopharmaceutics. 2014;**86**:7-22. DOI: 10.1016/j. ejpb.2013.08.013

[70] Glassman PM, Muzykantov VR. Pharmacokinetic and pharmacodynamic properties of drug delivery systems. The Journal of Pharmacology and Experimental Therapeutics. 2019;**370**: 570-580. DOI: 10.1124/jpet.119.257113

[71] Nguyễn CH, Putaux JL, Santoni G, Tfaili S, Fourmentin S, Coty JB, et al. New nanoparticles obtained by co-assembly of amphiphilic cyclodextrins and nonlamellar single-chain lipids: Preparation and characterization. International Journal of Pharmaceutics. 2017;**531**:444-456. DOI: 10.1016/j. ijpharm.2017.07.007

[72] Luque-Alcaraz A, Lizardi-Mendoza J, Goycoolea FM, Higuera-Ciapara I, Argüelles-Monal W. Preparation of chitosan nanoparticles by nanoprecipitation and their ability as a drug nanocarrier. RSC Advances. 2016; **6**:59250-59256. DOI: 10.1039/ c6ra06563e

[73] Lazzari S, Moscatelli D, Codari F, Salmona M, Morbidelli M, Diomede L. Colloidal stability of polymeric nanoparticles in biological fluids. Journal of Nanoparticle Research. 2012; **14**:920-930. DOI: 10.1007/s11051-012-0920-7

[74] Rodriguez-Emmenegger C, Jäger A, Jäger E, Stepanek P, Alles AB, Guterres SS, et al. Polymeric nanocapsules ultra stable in complex biological media. Colloids and Surfaces B: Biointerfaces. 2011;**83**:376-381. DOI: 10.1016/j.colsurfb.2010.12.013

[75] International Council for Harmonisation of Technical Requirements for Pharmaceuticals for Human Use. Impurities: Guideline for residual solvents Q3C (R6). 2016